Bioactive effects of natural and novel unnatural tropolone sesquiterpenoids in a murine cell model of renal interstitial fibroblasts

Timna Claire Bergmann, Max Menssen, Carsten Schotte, Russell J. Cox, Cornelia Lee-Thedieck

T.C. Bergmann, Prof. Dr. C. Lee-Thedieck

Institute of Cell Biology and Biophysics, Department of Cell Biology, Leibniz University Hannover, 30419 Hannover, Germany

bergmann@cell.uni-hannover.de

Corresponding Author E-mail: lee-thedieck@cell.uni-hannover.de

Dr. M. Menssen

Institute of Cell Biology and Biophysics, Department of Biostatistics, Leibniz University Hannover, 30419 Hannover, Germany

menssen@cell.uni-hannover.de

Dr. C. Schotte, Prof. Dr. R.J.Cox

Institute of Organic Chemistry and BMWZ, Leibniz University Hannover, 30167 Hannover, Germany

schotte.carsten@gmail.com

russell.cox@oci.uni-hannover.de

Keywords: tropolone sesquiterpenoids, synthetic biology, bioactivity, proliferation, cytotoxicity, erythropoietin

Abstract

Fungal specialized metabolites often exhibit a wide range of potent bioactivities, with tropolone sesquiterpenoids (TS) representing a promising family with a variety of known bioactive properties. Here, we investigated bioactive properties of the novel TS compounds 4-hydroxyxenovulene B **4**, 4-dehydroxy-norpycnidione **5** and the structurally-related compounds 4-hydroxy-norxenovulene B **6**, and xenovulene B **3**, for which no bioactive effects have been reported yet. We detected compound-specific changes in cell shapes and ramification patterns that were strongly correlated in samples treated with structurally-similar compounds and related to the tropolone moieties present on the molecule. The number of tropolone moieties per molecule had a significant influence on survival of FAIK3-5 cells, with an increased cytotoxic effect observed with the dual-substituted compounds compared to the monotropolones**.** Treatment with eupenifeldin **2**, compound **4** and **5** demonstrated versatile influences on cellular behaviour and can reduce EPO content in hypomethylated FAIK3-5 cells. Monotropolone **5** showed significantly reduced proliferation with low cytotoxic effects and could serve as a potential compound for further (pre-)clinical drug testing for cancer treatment. Our results bring us one step closer to linking the molecular structures of bioactive TS compounds to their biological effects and may improve their potential for clinical applications.

1. Introduction

Due to their diverse chemical architectures and structural complexity, natural products and their structural analogues have always been a valuable source of medical products. Dependent on fundamental functions for host survival and growth, these active ingredients are categorized into primary (amino acids, fatty acids and sugars) and secondary (or specialized) metabolites, which often display potent bioactivities [1, 2]. Natural specialized metabolites display a very broad range of diversity and they are often structurally optimized for particular biological

functions, which may have arisen, for example, from host defense mechanisms as a result of the reciprocal evolution of interacting hosts and their pathogens.

In recent years, advances in screening, isolation and characterization methods of these metabolites led to the discovery and development of novel drugs against a variety of infectious and cardiovascular diseases [3, 4], neurodegenerative diseases [5, 6] and cancer [7, 8]. Moreover, some of them have been shown to counteract against drug-resistant bacterial, fungal, viral or parasitic infections [9, 10], thereby demonstrating the great potential of natural products to target persistent challenges of medical care. Nonetheless, despite the recent progress in the development of innovative screening and characterization strategies, the number of unexplored compounds, or known compounds with unknown medical properties is still considered to be high, especially in fungi. For example, more than 1500 novel metabolites or families of metabolites with a wide range of biological activities were described between 1993 and 2001 [1] and the number of annually discovered fungal compounds dramatically increased from 655 in 2011 to 1236 in 2020 [11].

One promising family of fungal specialized metabolites are tropolone sesquiterpenoids (TS). These compounds boast an impressive spectrum of biological activities and potential pharmacological applications. In 1993 the bistropolone pycnidione **1** [12] and its diastereomer eupenifeldin **2** [13] were the first reported TS compounds and a wide variety of diverse biological activities for both compounds have been described since then. However, the exact determination of the stereochemistry has been difficult and has only recently been accurately reassigned [14, 15]. Following its isolation from *Eupenicillium brefeldianum* as an antitumor agent against human HTC colon carcinoma cell lines [13], further cytotoxic effects of eupenifeldin **2** were recorded for oral human epidermal carcinoma (KB) cells, human breast cancer (BC) cells, African green monkey kidney fibroblasts (Vero) cell lines, human small cell lung cancer (NCI-H187) cells, [16], Lewis lung carcinoma (LLC) and human lung carcinoma (A549) cells [17]. Furthermore, eupenifeldin **2** can be used as an antifungal (against *Candida*

albicans) and as an antimalarial compound (against *Plasmodium falciparum* K1) [16]. Similarly, reported activities of the structurally related TS compound pycnidione **1**, first isolated from an unidentified *Phoma* sp. [12], include anticancer activities against epidermoid carcinoma (KB), human breast cancer cells (BC-1) [18], the human T-cell leukemia-derived Jurkat cell line [19] and human lung cancer (A549) cells [20], as well as weak antibacterial [21] and antimalarial properties [18, 21, 22]. Additionally, pycnidione **1** is part of the "epolone family" of TS, known for the induction of erythropoietin (EPO) gene expression in HRCHO5, HepG2 and Hep3B reporter cell lines [23, 24]. Over the last decades a variety of bioactivities of other TS compounds, most of which belong to the eupenifeldin series, has been discovered [25–29], however, no such activities have been reported yet for the monotropolones xenovulene B **3,** first reported in 1997 [30] and fully characterized by Schor et al. [31], and 4-hydroxyxenovulene B **4** [32].

Structurally, TS compounds belong to a distinctive class of fungal meroterpenoids that share a conserved core structure comprising a humulene-derived 11-membered macrocycle and mono- or disubstituted pendent tropolones that are connected to the core via one or two dihydropyran rings (Fig. 1). Chemical diversity occurs naturally in TS metabolizing fungi, due to variances in distinct sets of fungal biosynthetic gene clusters (BGCs), which include most of the genes that encode metabolite synthesis. Redesign and refactoring of known BGCs and effective heterologous expression in pre-engineered hosts such as *A. oryzae* NSAR1, allows the acceleration of the synthesis process of TS compounds and enables the construction of platforms for new compound discovery. Thereby, the combination of genes of known BGCs can lead to a variety of new specialized metabolites with specific characteristics and putative bioactivities [33]. Previously, Schotte et al. described the successful isolation and identification of several TS compounds, including xenovulene B **3**, 4-hydroxyxenovulene B **4** as well as the two hitherto unknown compounds 4-dehydroxy norpycnidione **5** and 4-hydroxy norxenovulene B **6** by mixing and recombining genes of three key TS BGC in *A. oryzae* NSAR1 [31, 32]. To

date, no biological activity of these compounds has been reported in the literature but given the high potency of structurally related TS compounds such as pycnidione **1** and eupenifeldin **2**, similar effects on cellular mechanisms can be expected.

Bioactivity evaluation is a multi-step process that begins with the sole identification of active compounds by using *in vitro* assays to measure their primary activities (e.g. influences on cell growth or metabolic activity), selectivity, cellular toxicity, and physiologically relevant effects. Considering the wide range of influences that TS can have on cells, an appropriate platform that addresses the most important issues must be carefully selected. One of the most interesting physiological effects of TS compounds is the hypoxia-independent activation of EPO gene expression observed in the reporter cell lines Hep3B (Cai et al. 1998), HepG2, and HRCHO5 (Wanner et al. 2000) after treatment with pycnidione **1**. However, many early drug discovery studies rely on indirect measurements like luciferase reporter technologies, which can lead to false-positive results due to the occurrence of "frequent hitters" or other types of assay interferences [34], or are performed in genetically engineered cell lines that cannot reflect the physiological conditions of EPO production and regulation *in vivo*. To circumvent these problems and improve the quality of early *in vitro* drug testing studies, analysis of protein expression in a system more similar to natural conditions would be beneficial and lead to more reliable results. Physiologically, EPO is mainly produced by fibroblastoid renal erythropoietin-producing cells (REPs) and is highly regulated at the transcriptional level, but its production is also dependent on external factors like the decrease of tissue O_2 pressure and epigenetic mechanisms [35]. Therefore, and since EPO regulatory mechanisms are complex and not yet fully understood, a sustainable and simplified model for EPO *in vitro* studies is desirable. Recently, Imeri et al. introduced an immortalized clonal cell line derived from mouse REP cells called FAIK3-5 that can produce erythropoietin for at least 30 passages [36]. By using this cell line to test the bioactivity of the newly discovered TS and related compounds [32] (Fig. 1), we

are closer to a physiological model than when using cell lines derived from liver tissue and also meet the necessary requirements for toxicological and cell proliferation studies.

Furthermore, in the course of lead identification, morphological profiling is a meaningful indicator to assess whether the tested compounds can cause morphological changes associated with cell adhesion, proliferation behaviour or cell viability [37–39]. Cellular morphology is a function of dynamic interactions and balance between a series of physical forces exerted to the cytoskeleton, cell membrane and adhesion complexes that interact with the extracellular matrix. Regulatory signal transduction systems can convert these external cues into biochemical signals necessary for the cells' adaptation to environmental changes [40]. Cell phenotypes therefore combine observable characteristics with biochemical properties and gene and protein expression. However, to mitigate the effects of subjective evaluation of visual analysis, standardized morphometric descriptors and analysis tools are needed that can reveal information not readily apparent from a cursory visual inspection [41].

Therefore, in this study we used previously described standardized morphometric and two-dimensional branching descriptors to identify specific differences in cell shapes and ramification patterns [41, 42] between murine REP derived FAIK3-5 cells treated with the novel TS compounds 4-hydroxyxenovulene B **4** and 4-dehydroxy norpycnidione **5**, as well as with the structurally related compound 4-hydroxy norxenovulene B **6** and xenovulene B **3**, for which no bioactive effects have been reported yet. By comparison with characterized bioactive compounds such as eupenifeldin **2** and pycnidione **1**, and in combination with viability, proliferation, and protein expression assays, we aim to find a link between the molecular structures of related TS compounds and their biological effects. This knowledge will help to decipher the biological functions of TS moieties and can support approaches in synthetic biology for redesigning TS compounds. In this way medical needs can be targeted by increasing drug efficacy while mitigating undesirable side effects, thereby improving their potential for further clinical applications.

2. Materials and Methods

2.1. Biosynthesis of tropolone-sesquiterpenoid compounds

Pycnidione **1** and eupenifeldin **2** were isolated respectively from *Leptobacillium* sp. CF-236968 and *Phaeosphaeriaceae* sp. CF-150626 (formerly referred to as unidentified ascomycete F-150626) that naturally produce the compounds. For the heterologous production of the described tropolone sesquiterpenoid (TS) compounds **3-5** and control compound 4-hydroxy norxenovulene B **6**, a series of TS key biosynthetic gene clusters (BGC) were refactored and recombined in *A. oryzae* NSAR1 as previously described by Schotte et. al [32]. The currently accepted stereochemistry of these compounds is displayed in Fig. 1[14].

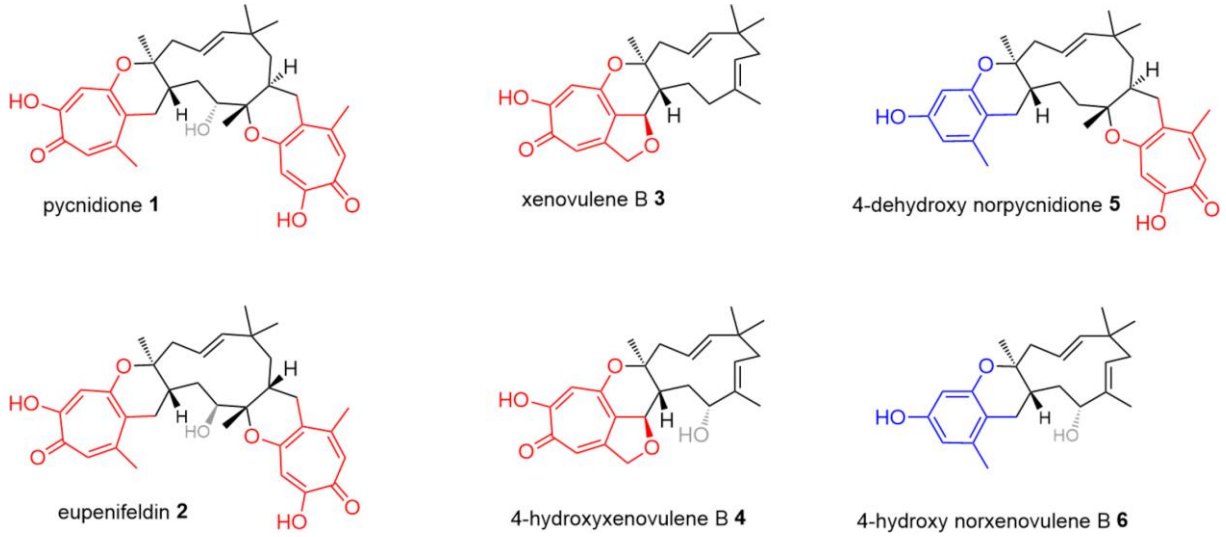

Fig. 1: Stereochemistry of selected tropolone sesquiterpene (TS) compounds (**1-5**) and control compound (**6**) lacking a tropolone moiety [14]. Key features are highlighted in red (= polyketide derived tropolones), blue (= benzopyranyl moiety) and grey (C-10 hydroxylation).

2.2. Biosynthesis of tropolone-sesquiterpenoid compounds

Fibroblastoid atypical interstitial kidney (FAIK) 3-5 cells were obtained from the Leibniz Institute DSMZ-German Collection of Microorganisms and Cell Cultures GmbH

(Braunschweig, Germany) and were cultured according to the recommended culturing protocol in Dulbecco′s Modified Eagle′s Medium (DMEM) - high Glucose (Sigma Aldrich, St. Louis, MO, United States) supplemented with 10 % FBS (Sigma Aldrich, St. Louis, MO, United States; Lot: BCBW9923), which is referred to in the following as cell culture medium. As the cell line was previously described to produce EPO protein for at least 30 passages [36], all experiments were conducted on cells below that passage number. Cells were split every two to three days and at a confluency of 80 – 90 %.

2.3. Compound reconstitution and TS treatment of FAIK3-5 cells

Lyophilized TS compounds were reconstituted in dimethylsulfoxid (DMSO, Carl Roth GmbH, Karlsruhe, Germany) to obtain 1 mM stock solutions, sterile filtered and stored at -20 °C until further use. To maintain compound stability, repeated freeze-thaw cycles of compound aliquots were avoided. For the investigation of TS compound influence on FAIK3-5 cells, 5×10^{5} cells / well (6well, CellStar™, Greiner Bio-One, Kremsmünster, AT) were seeded and kept in culture for 24 h, before cell adherence and morphology were assessed visually. Prior to TS treatment FAIK3-5 cells were washed thoroughly with Dulbecco's Phosphate Buffered Saline (DPBS) (Sigma Aldrich, St. Louis, MO, United States) and incubated with 4-12 µM TS compound containing cell culture media for another 24 h. For subsequent experiments with compound treated cells, respective DMSO vehicle controls and untreated medium controls were used.

For the determination of EPO concentrations FAIK3-5 cells were treated with TS compounds, respective vehicle controls (0.6 % *v/v* and 1.2 % *v/v* DMSO) or not treated for 24 h as described above and cell extracts were analysed for EPO protein concentrations. It is known that the physiological EPO production is tightly controlled by an "on-off" regulatory behaviour of REP cells and by DNA methylation in the *EPO*-gene promoter that can cause the loss of EPO production capability in REP cells [49]. Therefore, FAIK3-5 were treated with 1 µM of the

hypomethylating agent 5-Azacytidine (5-Aza, Sigma-Aldrich, St. Louis, MO, United States) in an additional approach. The treatment was conducted for six days with complete medium changes every other day to ensure sufficient cell divisions for 5-Aza integration and agent replenishment before degradation. After this period the cells were treated with TS compounds and vehicle controls (0.6 % *v/v* and 1.2 % *v/v* DMSO) and EPO protein content was measured.

2.4. Morphological analysis

In order to handle environmental changes, cells possess the ability to attain a more desirable stress state by the activation of distinct molecular pathways, which morphologically might lead to profound changes of cell shapes. To analyse different morphological shapes of FAIK3-5 cells caused by TS compound treatment, brightfield pictures were taken with a ZEISS Axio Vert.A1 Inverted Microscope (Zeiss, Oberkochen, Germany) 24 h after TS treatment and directly before subsequent analysis of the cells.

For each treatment condition at least 20 cells from three independent experiments were analysed for morphological changes with Fiji (ImageJ, Version 1.53c bundled with Java 1.8.0_172) [61]. The results were visualized using OriginPro 2021 (Version 9.8.0.200) and the Matlab (Version R2021b) toolbox PhenoPlot [44], an open source visualization tool for imaging data that is able to represent multiple dimensions of cellular morphology as intuitive cell-like glyphs. To obtain the most accurate illustration of different cell shapes, regions of interest (ROIs) were drawn by hand and basic morphometric variables (cell area, perimeter, major and minor axis) and standard shape descriptors (circularity, aspect ratio, roundness and solidity) were measured in Fiji. To analyse differences in ramification patterns of cells treated with distinct TS compounds two-dimensional branching descriptors were calculated using the AnalyzeSkeleton plugin [42]. For a detailed description of morphological analysis and PhenoPlot visualization see Fig. S1.

2.5. Proliferation and Cytotoxicity Assay

To evaluate effects of proliferative behaviour and cell viability caused by TS compounds, FAIK3-5 cells were cultured in cell culture medium as described above and labelled with the CellTrace™ Violet (CTV) Cell Proliferation Kit (Invitrogen, ThermoFisher Scientific, Waltham, MA, United States) at a concentration of 10 µM CTV per 1×10^{6} cells according to the manufacturer's protocol with minor modifications. To assure homogenous CTV labelling, 900 µl of cell suspension containing 1×10^{6} cells were kept in a 15 mL tube (Greiner Bio-One, Kremsmünster, Austria), which was positioned horizontally before 100 µl of CTV staining solution was added to the upper end of the tube without mixing. The tube was kept in that position until the lid was closed carefully, and mixing was conducted on a vortex mixer (Benchmark Scientific, Sayreville, NJ, United States). After 20 minutes of staining at 37 ° C in the dark, the reaction was stopped by adding 5 times the original staining volume of DPBS with 10 % of FBS and incubation for 5 minutes on ice to remove unbound dye particles. Subsequently, the supernatant staining solution was removed after centrifugation at 300 × g for 5 minutes, and FAIK3-5 cells were counted and seeded into 6-well plates (Greiner Bio-One, Kremsmünster, Austria) with a cell density of 5×10^{5} cells per well. Cell viability was evaluated via SYTOX™ AADvanced™ Dead Cell Stain Kit (Invitrogen, ThermoFisher Scientific, Waltham, MA, United States) staining according to the manufacturer's instructions prior to analysis with the BD FACSverse™ Cell Analyzer (BD, Franklin Lakes, NJ, United States) cytometer.

Directly after staining, cell samples were analysed with the flow cytometer to ensure homogenous dye distribution within the population and to monitor cell viability after the staining process. For each analysed sample 10 000 events were counted. Gating strategies for living/dead discrimination and proliferation analysis are explained in more detail in the Supporting Information section (Fig. S2 A and B). For each analysis unstained cells, CTV-

stained cells without compound treatment and live/dead control samples, comprising a heat-killed population to set the fluorescence threshold for live/dead discrimination, were included as staining controls. To assess the optimal analysis period for the CTV proliferation tests, untreated FAIK3-5 cells were analysed via flow cytometry for CTV intensities and putative effects of the CTV staining on cell viability on three subsequent days in preliminary experiments (Fig. S2 B-D).

For following experiments with compound treated samples, measurements were taken at day 1 (d1) to obtain the basic CTV intensities of the stained samples. At day 2 TS compound treatment was started and at day 3 (d3), after 24 h of incubation, the second measurement was conducted to evaluate changes in CTV intensities after TS treatment. For each experiment untreated cells and vehicle controls (0.6 % v/v and 1.2 % v/v DMSO) were included as treatment control samples. After cellular uptake by diffusion, CTV covalently binds to intracellular amines and is diluted proliferation dependently within the analysed cellular populations. However, as the cellular uptake and binding capacity is contingent on multiple factors (e.g. cell viability, division stage or cellular protein level), a perfectly homogenous staining throughout experimental repetitions is not possible and hence result in distinct MFIs at d1 of the experiments. Accordingly, for statistical analysis obtained values were normalized by calculating the proportions of measured MFIs at the beginning (d1) and end (d3) of the experiments and pairwise mean comparison tests were run based on mean differences. For descriptive statistics mean values and standard deviations were obtained from the calculated fold changes enlisted in Table S5.

3. Results

3.1. Structurally related tropolone sesquiterpenoids promote similar morphological alterations in FAIK3-5 cells

Substantial alterations in cell morphologies are frequently observed during screening studies of natural or synthetic compounds [37, 43]. Correspondingly, changes in cell morphologies of TS compound treated samples compared to untreated control samples were also observed in this study, correlating in samples treated with compounds with structural similarity.

Microscopic examinations on FAIK3-5 cells were conducted 24 h after treatment with different TS and structurally related compounds in concentration ranges of 4 to 12 µM (Fig. S3). Compound treatment showed either no effect on cell growth and morphology (4-hydroxy norxenovulene B **6**), or a prominent modification of cellular shapes in a dose-independent manner after treatment with tropolone-bearing compounds (pycnidione **1**, eupenifeldin **2**, xenovulene B **3**, 4-hydroxyxenovulene B **4** and 4-dehydroxy norpycnidione **5**). Samples treated with 4-hydroxyxenovulene B **4** additionally revealed lower cell confluency at a concentration of 12 µM compared to samples treated with lower concentrations (4 to 6 µM).

Treatment with the two included bistropolones pycnidione **1** and its diastereomer eupenifeldin **2**, induced a neuron-like morphology with highly ramified cell protrusions in FAIK3-5 cells, while treatment with the monotropolones xenovulene B **3**, 4-hydroxyxenovulene B **4** and 4-dehydroxy norpycnidione **5** resulted in an epithelial-like cell morphology. 4-hydroxy norxenovulene B **6** treated cells displayed a more elongated, fibroblast-like morphology that resembles the natural morphology of FAIK3-5 cells visible in untreated control samples. Furthermore, the emergence of flat and enlarged cells, which were highly granulated, was observed in all treatment conditions with tropolone-containing compounds (**1-5**) (Fig. 2 A). Notably, the tropolone lacking compound 4-hydroxy norxenovulene B **6** showed no alteration in cell morphology or growth inhibition, indicating that especially the tropolone moieties of the

tested compounds are responsible for alterations in cell phenotypes, viability and proliferative behaviour of the cells (Fig. S3).

Based on this observation we hypothesized that treatment with structurally related TS compounds might trigger similar biochemical responses in FAIK3-5 cells, thereby inducing comparable phenotypes. To test this hypothesis multiple comparison tests on shape descriptors and morphometric parameters (cell area, aspect ratio (AR), perimeter, relative protrusion area (= solidity), length of protrusions (= circularity) as well as number of protrusions and branches) were performed to detect putative morphological similarities between the TS-treated cells (Fig. 2 B). As all applied statistical analysis models depend on variables that were measured on the same cell, multiple contrast tests were carried out with respect to the correlations between dependent variables using multiple marginal models (Supporting Information S9 and S10). For the sake of better visualization of the morphological appearance of cells, differently treated and untreated FAIK3-5 samples were illustrated with the Matlab (Version R2021b) toolbox PhenoPlot [44]. Visualized plots concur with the conducted multiple comparison analysis (Fig. 2 C), which reveal no significant differences ($p > 0.05$) of cell area, aspect ratio (AR), perimeter, relative protrusion area, length and number of protrusions as well as for the number of cell branches and junctions in samples treated either with the bistropolones pycnidione **1** and eupenifeldin **2**, or with the monotropolones xenovulene B **3** and 4-hydroxyxenovulene B **4**. Contrarily, the treatment with unrelated compounds led to significant morphological differences between analysed cell samples. Cells treated with compound 4-dehydroxy norpycnidione **5**, which belongs to the xenovulene-/ pycnidione-type TS, characterized by the trans-fusion at C-8/C-9 position of the central α-humulene derived macrocycle, show a higher morphological equivalence to cells treated with the structurally distinct TS compounds xenovulene B **3** and 4-hydroxyxenovulene B **4** than to any of the other investigated compounds. Cells treated with 4-dehydroxy norpycnidione **5** are significantly morphologically altered only in regard of their measured AR ($p \leq 0.001$), whereas 4-hydroxyxenovulene B **4** treatment

additionally induces significant changes in cell area ($p \leq 0.001$) and length of protrusions ($p \leq 0.05$).

With this we can show that observed alterations in cell growth and morphology strongly relate to the tropolone moieties present on the molecules, which seem to be responsible for their bioactivity. This is additionally validated by the lack of biological responses after 4-hydroxy norxenovulene B **6** treatment and the high morphological similarity of mono- and bistropolone treated cells.

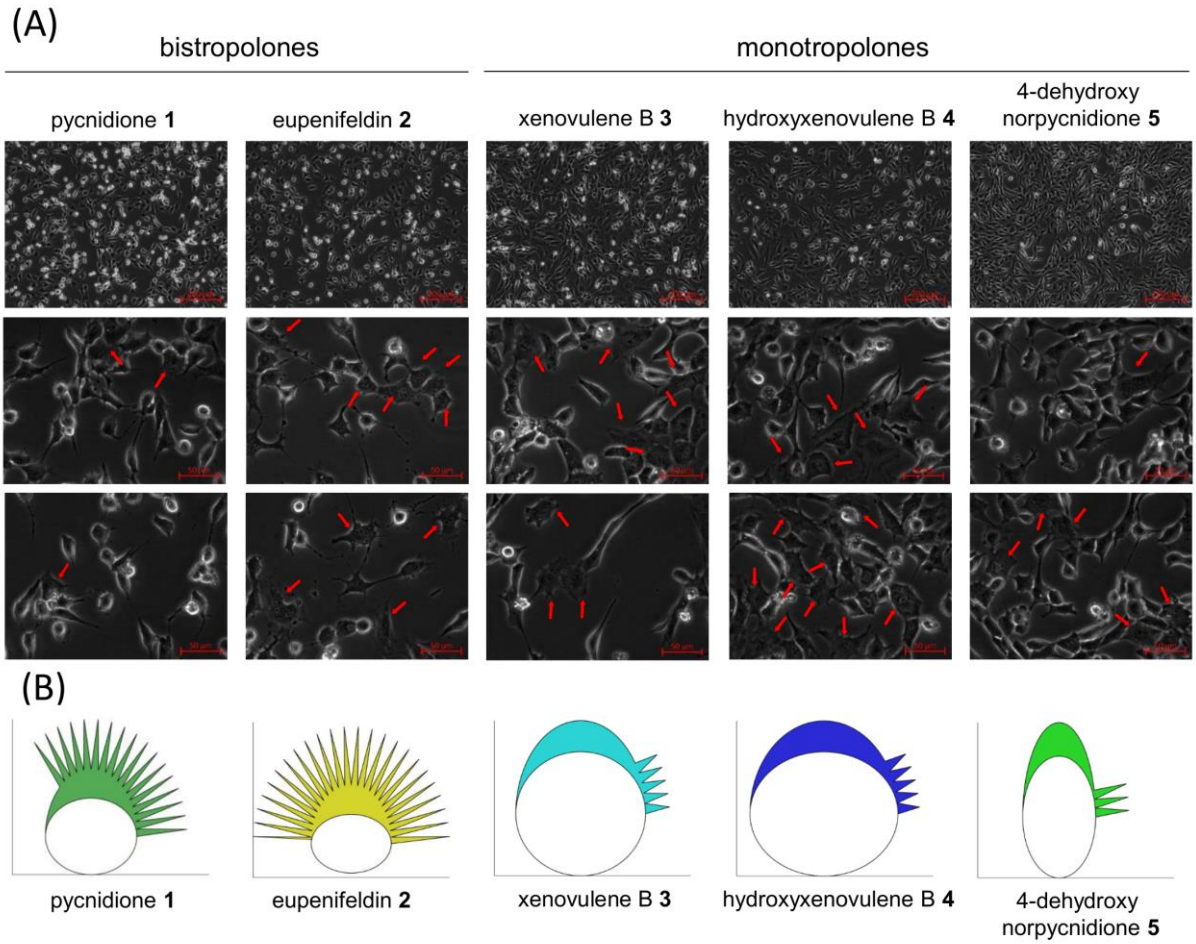

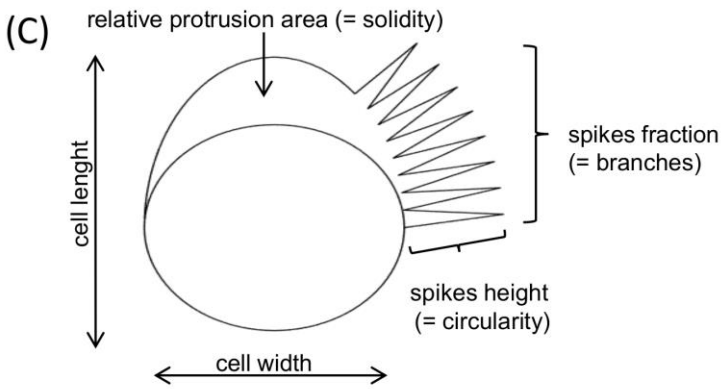

	cell area†	aspect ratio	perimeter†	solidity	circularity = length of protrusions	branches = number of protrusions	junctions†
xenovulene B **3** vs. eupenifeldin **2**	NS	NS	***	***	***	***	***
xenovulene B **3** vs. 4-dehydroxy norpycnidione **5**	NS	***	NS	NS	NS	NS	NS
xenovulene B **3** vs. hydroxyxenovulene B **4**	**NS**	**NS**	**NS**	**NS**	**NS**	**NS**	**NS**
xenovulene B **3** vs. pycnidione **1**	NS	NS	***	***	***	***	***
eupenifeldin **2** vs. 4-dehydroxy norpycnidione **5**	*	***	***	***	**	***	***
eupenifeldin **2** vs. hydroxyxenovulene B **4**	NS	NS	***	***	***	***	***
eupenifeldin **2** vs. pycnidione **1**	**NS**	**NS**	**NS**	**NS**	**NS**	**NS**	**NS**
4-dehydroxy norpycnidione **5** vs. hydroxyxenovulene B **4**	***	***	NS	NS	*	NS	NS
4-dehydroxy norpycnidione **5** vs. pycnidione **1**	NS	***	***	***	*	***	***
hydroxyxenovulene B **4** vs. pycnidione **1**	***	NS	***	***	***	***	***

Fig. 2: Alterations of cell morphology of FAIK3-5 cells after 24 h of treatment with the TS

compounds pycnidione 1, eupenifeldin 2, xenovulene B 3, 4-hydroxyxenovulene B 4 and 4-dehydroxy norpycnidione 5. (A) Brightfield images (1 x 10x and 2 x 20x resolution from top to bottom) of samples treated for 24h with compound 1-5. Red arrows indicate enlarged, flat and highly granulated cells that were visible to varying degrees in each treated sample. (B) Visualization of TS-treated cells in PhenoPlot, in which quantifiable cell features such as cell width and length, relative area of protrusions as well as their proportion and size (spike fraction and spike height) are displayed for each sample condition. In order to emphasize main differences between different treatments relative protrusion areas, spike fractions and spike height are coloured in dark green (pycnidione 1), yellow (eupenifeldin 2), light blue (xenovulene B 3), dark blue (4-hydroxyxenovulene B 4) and light green (4-dehydroxy norpycnidione 5). (C) Multiple comparison analysis for analysed shape descriptors and morphometric parameters (cell area, aspect ratio, perimeter, relative protrusion area as well as length and number of protrusions/branches and branch junctions) were measured on at least 20 cells of pictures from three independent experiments in Fiji (version 1.53c). Statistical analysis of data was conducted with R (version 4.2.1). All parameters marked with (†) are not depicted in PhenoPlot graphs. Significances range from $p > 0.05$ (NS), 0.05 - 0.01 (*), < 0.01 - 0.001 (**) to < 0.001 (***). The estimated contrasts and corresponding confidence intervals are given in Supporting Information S 9 and S 10.

3.2. Tropolone moieties induce a downshift of cell proliferation and increased cytotoxicity upon dual-substitution

Rearrangements of the cytoskeletal architecture yielding morphological distortions such as e.g. irregular cell shapes, micronuclei formation and an extended protrusion area might indicate cytotoxic cell responses, but can also be a sign for putative cytostatic effects and diminished proliferative behaviour [43, 45, 46]. As the cell morphology was demonstrably altered in

samples treated with TS compounds, we aimed to analyse if these changes are accompanied by proliferative inhibition, which was described before for pycnidione-treated lung cancer cells [20]. Therefore, effects of TS compound treatment on proliferation and cytotoxicity were assessed in CTV stained FAIK3-5 cells. For this purpose, we evaluated the concentration dependency of the putative proliferation inhibition effects of chosen compounds via incubation of FAIK3-5 cells with TS compounds at 4 µM, 6 µM, 8 µM and 12 µM for 24 h and subsequent analysis of mean fluorescence intensity (MFI) decrease caused by the proliferation dependent loss of incorporated CTV molecules (Fig. S2 and Table S5). For pycnidione **1**, eupenifeldin **2**, xenovulene B **3** and 4-dehydroxy norpycnidione **5** we observed proliferative deceleration of FAIK3-5 cells, discernible by increased MFI values (2.26 ± 0.4-fold higher) compared to the untreated control samples, which was independent of the applied concentration. For 4-hydroxyxenovulene B **4,** a dose-dependent decrease of proliferation in treated cells, with the highest decline at a compound concentration of 12 µM (2.62-fold higher) compared to untreated samples, was observed (Table S5). The tropolone-moiety lacking compound 4-dehydroxy norxenovulene B **6** showed no evidence of bioactivity in terms of proliferation inhibition in FAIK3-5 cells after 4 µM and 6 µM treatment compared to the untreated control. A slight but significant decrease in cell growth was observed in samples treated with 8 µM ($p = 0.027$) and 12 µM ($p = 0.001$) of 4-dehydroxy norxenovulene B **6** (Fig. S6, Table S5 and Supporting Information S11). To exclude potential solvent effects, an analysis was conducted with DMSO vehicle controls in the respective concentration accessible to cells during compound treatment (0.4 % (*v/v)*, 0.6 % (*v/v*), 0.8 % (*v/v*) and 1.2 % (*v/v*)) and compared to untreated controls and the tropolone-moiety lacking compound 4-hydroxy norxenovulene B **6,** which did not trigger an observable morphological alteration or growth inhibition of treated FAIK3-5 cells (Fig. S3 and Fig. S6). We could not observe significant effects on the proliferative behaviour of cells treated with DMSO compared to the respective concentrations of compound **6**. However, effects on cell growth were observed in samples treated with 1.2 % (*v/v*) DMSO or 8 - 12 µM

4-hydroxy norxenovulene B **6** compared to untreated samples. Nevertheless, the percentage of proliferation deceleration was rather small in both the vehicle control (8.64 ± 3.72 % after 1.2 % (*v/v*) treatment), and tropolone-lacking compound treated samples (4.91 ± 4.43 % after 8 µM treatment and 7.64 ± 3.66 % after 12 µM treatment) compared to samples treated with TS compounds (129.95 ± 37.88 % and 143.52 ± 41.78 %) in the respective concentrations (Table S5).

Based on the observed effects of the different applied concentrations, following comparative experiments focused on differences in proliferative behaviour of FAIK3-5 cells treated with TS compounds (**1**-**5**), tropolone lacking compound **6** or DMSO vehicle controls in defined concentrations. Selected treatment concentrations were chosen at 6 µM for both bistropolones pycnidione **1** and eupenifeldin **2**, as well as for the monotropolone xenovulene B **3**, and 12 µM for the monotropolones 4-dehydroxy norpycnidione **5** and 4-hydroxyxenovulene B **4** and emanate from previous studies [23, 24] and the effects observed in preceding experiments (Fig. S1 and S2 and Table S3). All analysed TS compounds led to a significantly decreased proliferation rate in treated cells ($p < 0.001$) compared to the untreated control as shown by their low MFI values compared to the untreated control samples (Fig. 3 A) and shifts to lower fluorescence intensities in the respective flow cytometry histograms (Fig. 3 B). The tropolone moiety lacking compound 4-hydroxy norxenovulene B **6** had no measurable effect on FAIK3-5 growth compared to untreated control samples ($p = 0.951$) and showed a significant difference in MFI values compared to all samples treated with TS compounds ($p > 0.001$) (Fig. 3 A, C). Moreover, as there were no detectable differences between the different analysed TS compounds (Fig. 3 B), these results strongly indicate a key role of the tropolone-moiety in proliferation inhibition, independent of its single or dual substitution to the central 11-membered α-humulene-derived core structure of the compounds.

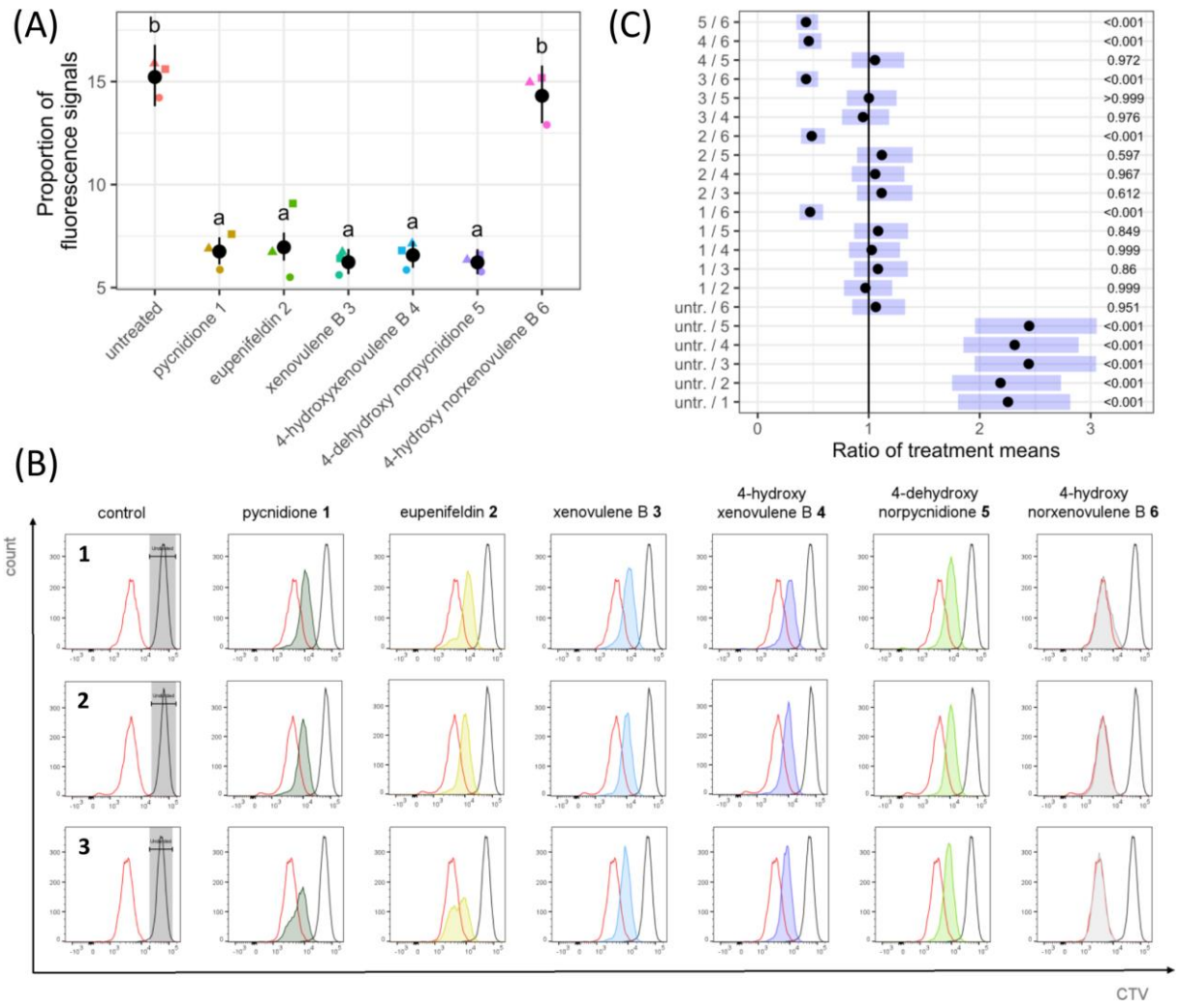

Fig. 3: Proliferation deceleration of FAIK3-5 cells after treatment with pycnidione **1**, eupenifeldin **2**, xenovulene B **3**, 4-hydroxyxenovulene B **4** and 4-dehydroxy norpycnidione **5** compared to untreated controls and tropolone moiety lacking compound 4-hydroxy norxenovulene B **6**. Statistics were calculated based on normalized values of obtained ln-transformed mean fluorescence intensities (MFIs) directly after cell trace violet (CTV) staining of the undivided population and 24h post compound treatment. (A) Graphical overview show normalized MFI values of three biological replicates (● = 1, ▲ = 2, ■ = 3) after treatment with compounds **1** - **6** and the untreated control sample, as well as their modelled means (black dots) and pointwise 95% confidence intervals. Treatments marked with the same letter do not differ significantly from each other (α = 0.05). (B) Histograms and obtained fluorescence intensities of CTV stained FAIK3-5 cells show MFI peaks and values of starting intensities of undivided

cell populations at d1 (grey background), control peaks of untreated samples at d3 (red) and MFI peaks of the respective compounds used for treatment (dark green = pycnidione **1**, yellow = eupenifeldin **2**, light blue = xenovulene B **3**, dark blue = 4-hydroxyxenovulene B **4**, light green = 4-dehydroxy norpycnidione **5**, 4 grey = 4-hydroxy norxenovulene B **6**). (C) Pairwise mean comparisons showed significant differences in normalized MFI values between all TS compounds treated cells compared to untreated controls and compound 4-hydroxy norxenovulene B **6**. Black dots indicate back transformed means of calculated ratios and their 95% confidence intervals (blue bars). Respective p-values for each calculation are displayed on the right side. The estimated contrasts and corresponding confidence intervals are given in Supporting Information S11 and S12.

For cytotoxicity assessment FAIK3-5 were treated for 24 h with the same concentrations of the compounds as described before, stained with the nucleic acid stain SYTOX™ AADvanced™ and analysed via flow cytometry.

In initial control experiments, putative effects of DMSO (0.4 % (*v/v*), 0.6 % (*v/v*), 0.8 % (*v/v*) and 1.2 % (*v/v*)) and the tropolone moiety lacking compound 4-hydroxy norxenovulene B **6** (4 µM, 6 µM, 8 µM and 12 µM) on FAIK3-5 cell survival were investigated and compared to untreated samples (Table S5 and Fig. S7). In this regard and for subsequent experiments, significances were calculated via pairwise mean comparison analysis on logit scale based on odds ratios calculated from the number of living and dead cells per analysed sample (sample size = 10.000 cells) after 24 h of treatment. These ratios represent the chance to obtain dead cells in a specific sample compared to the chance of obtaining dead cells in the respective correlated sample (Supporting Information S13 and S14). Compared to untreated medium controls, a significant increase of dead cells in DMSO and 4-hydroxy norxenovulene B **6** treated samples was measured at all tested concentrations (0.4 % (*v/v*) to 1.2 % (*v/v*) and 4 µM to 12 µM), however no dose-dependency could be observed (Table S5 and Fig. S7).

The measured viability in all samples ranged from 91.7 % to 99.8 %, which lies within the measured range of cell viability for untreated cultures of FAIK3-5 cells (89.9 – 97 %) (N = 7, data not shown) and is considerably higher than after treatment with the bistropolones pycnidione **1** (48.5 - 71.8 %) and eupenifeldin **2** (55.8 – 72.1 %) (Table S5).

Comparing the effects of the different analysed compounds on cell survival, we observed a significant increase in the proportion of dead FAIK3-5 cells upon treatment with pycnidione **1** ($p < 0.001$), eupenifeldin 2 ($p < 0.001$), xenovulene B 3 ($p = 0.012$) and 4-hydroxyxenovulene B 4 ($p = 0.004$), compared to the untreated controls (Fig. 4 A, B). By analysing the effect on cell survival compared to the tropolone lacking compound 4-hydroxy norxenovulene B 6 instead of untreated samples, FAIK 3-5 cells exhibited a highly increased proportion of dead cells after treatment with the bistropolones 1 and 2 ($p < 0.001$), but not after treatment with the monotropolones 3, 4 and 5. Thus, the inclusion of a second tropolone moiety to the TS-core structure seemed to have an additional effect on cell survival in vitro compared to monotropolone compounds, emphasized by the significantly lower amount of detected dead cells in samples treated with xenovulene B 3 compared to pycnidione 1 ($p = 0.036$). Anyhow, the lower confidence limit for this odds ratio is 1.031 and thus only slightly above one. Hence, this difference has to be interpreted with care. The monotropolone 4-dehydroxy norpycnidione 5 showed no significantly enhanced cell death compared to both, untreated controls and samples treated with the tropolone-lacking compound 4-hydroxy norxenovulene B 6. Accordingly, cell toxicity to FAIK3-5 cells was significantly lower than for both bistropolones ($p \leq 0.001$). Fig. 4 A, B).

All in all, our results show that the tropolone moieties present on the compounds significantly influence cell survival of FAIK3-5 cells, whereas increased cytotoxic effects were observed on dual-substituted compounds (**1** and **2**).

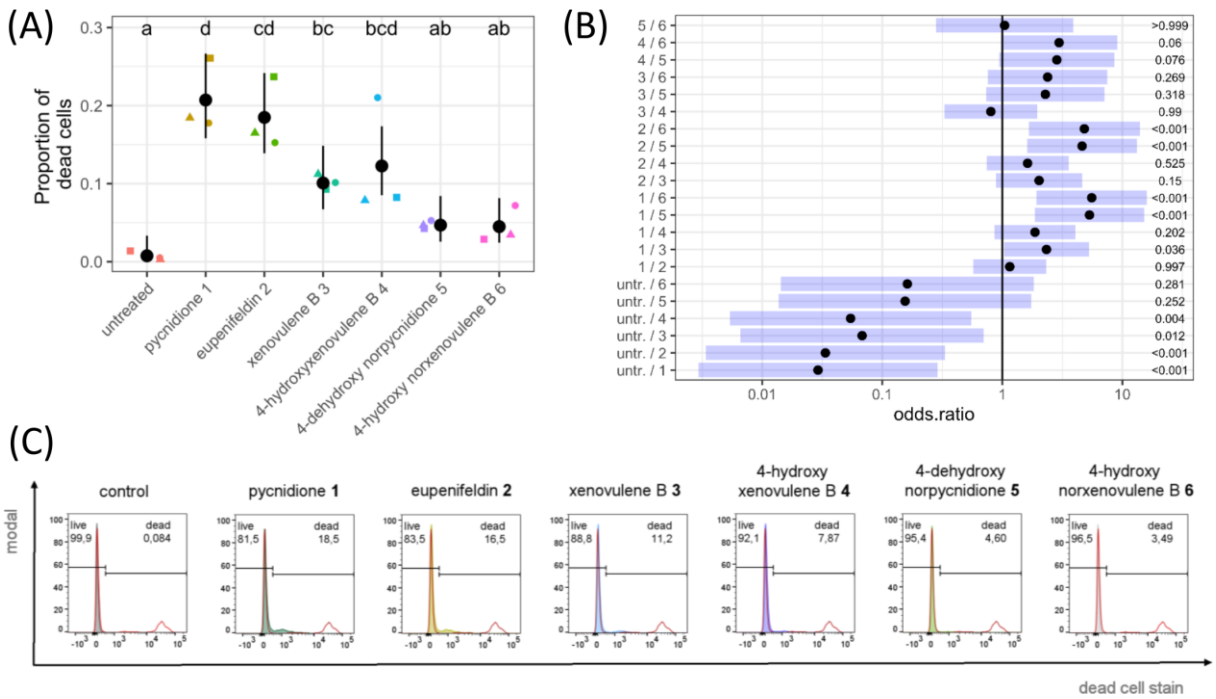

Fig. 4: Cell viability of FAIK3-5 cells after treatment with pycnidione **1**, eupenifeldin **2**, xenovulene B **3**, 4-hydroxyxenovulene B **4** and 4-dehydroxy norpycnidione **5** for 24 h and compared to untreated controls and tropolone moiety lacking compound 4-hydroxy norxenovulene B **6**. Statistical analysis was conducted based on the calculation of the average proportion of dead cells per samples (samples size = 10.000 cells). (A) Proportions of dead cells (black dots) and their pointwise 95 % confidence intervals (error bars) of three biological replicates (● = 1, ▲ = 2, ■ = 3). Treatments marked with the same letter do not differ significantly from each other (α = 0.05). (B) Multiple comparisons of calculated odds ratios (black dots) and simultaneous 95 % confidence intervals (blue bars, details see Supporting Information S14) showing differences of cell survival between samples treated with tropolone moiety containing compounds (**1** – **5**) compared to untreated samples or tropolone-lacking compound **6**. P-values for each contrast test of different treatments are displayed on the right side. (C) Representative plot of fluorescent intensities of SYTOX™ AADvanced™ stained FAIK3-5 cells samples. Each plot displays percentages of living and dead populations in an untreated control sample and after treatment with and the TS compounds pycnidione **1**, eupenifeldin **2**, xenovulene B **3** and 4-hydroxyxenovulene B **4** and 4-dehydroxy norpycnidione

5, and tropolone lacking compound 4-hydroxy norxenovulene B **6**. Peaks of fluorescence intensities are displayed with the respective living / dead control (red) containing a heat-killed dead cell population.

3.3. Tropolone-sesquiterpenoid compounds do not enhance erythropoietin protein production in a cell model for natural EPO production

Epolone-dependent induction of erythropoietin reporter gene activity and protein expression was described for several cell lines, such as HRCHO5 and Hep3B cells [23, 24], thereby leading to the assumption that specific TS compounds might play a role in the induction of EPO synthesis independent of oxygen availability. To analyse if the utilized compounds are capable to also stimulate the natural EPO-production in REP-derived FAIK3-5 cells *in vitro*, the EPO protein content of TS compound treated cell extracts was measured via ELISA.

To assess optimal compound concentration und putative concentration dependencies, compounds were administered to FAIK3-5 cells at 4 µM, 6 µM, 8 µM and 12 µM prior to EPO protein analysis (Fig. S8). In the following, pycnidione **1**, eupenifeldin **2**, xenovulene B **3** and the tropolone-lacking compound 4-hydroxy norxenovulene B **6** were utilized at an intermediate concentration of 6 µM, and 4-dehydroxy norpycnidione **5** was applied at 12 µM, where EPO production was higher in comparison to 6 µM. Treatment with different concentrations of 4-hydroxyxenovulene B **4** did not reveal a dose-dependent effect on EPO production in FAIK3-5 cells (Fig. S8), however, as REP cells usually are quiescent or show little proliferation capacity [47, 48] and due to the dose-dependent decrease in proliferation after 4-hydroxyxenovulene B **4** treatment (Fig. S4), we also chose a concentration of 12 µM for subsequent studies on EPO production.

We could not detect a determinable enhancing effect exerted by the utilized compounds on EPO concentrations in cell lysates. Moreover, we observed variability between biological replicates. (Fig. 5 A and Supporting Information S15). One possible reason could be epigenetic silencing of EPO synthesis by hypermethylation of the EPO promoter and regulatory gene sequences [49]. To circumvent this effect in FAIK3-5 cells, samples were treated with 1 µM of the hypomethylating agent 5-Azacytidine (5-Aza) for six days with complete medium changes every other day to ensure sufficient cell divisions for 5-Aza integration before compound treatment. As the vehicle control DMSO itself might support hypermethylation events within the cells [50], the effectiveness of 5-Aza treatment in enhancing EPO production of FAIK3-5 cells was assessed in DMSO vehicle controls (0.6% (*v/v*) and 1.2% (*v/v*)) and showed an increase in measured basic EPO concentrations (Fig. 5 B). The measured EPO protein content between biological replicates was more stable after 5-Aza treatment (Supporting Information S16). However, despite the general increase in EPO synthesis after 5-Aza administration, the additional treatment with TS- compounds showed no enhancing effect on EPO protein synthesis after hypomethylation compared to the respective vehicle controls (Fig. 5 C). In contrast, treatment with 4-hydroxyxenovulene B **4** ($p = 0.008$), 4-dehydroxy norpycnidione **5** ($p = 0.028$) and eupenifeldin **2** ($p = 0.046$) treatment significantly decreased the measured EPO protein content compared to the vehicle control. However, the effect of eupenifeldin **2** on 5-Aza treated FAIK3-5 cells was considered as marginal (Fig. 5D).

Summing up, contrary to previous findings describing an enhancing effect of pycnidione **1** on EPO gene expression in HRCHO5, HepG2 and Hep3B reporter cell lines [23, 24], we could not consolidate these results regarding an enhancing effect on EPO production in the REP cell line model after treatment with TS compounds **1** – **5** and the tropolone-lacking compound **6**, even though the compounds showed demonstrable bioactivity concerning cell growth inhibition and cytotoxicity. Moreover, three out of six tested TS compounds, namely the bistropolones eupenifeldin **2**, and the monotropolones 4-hydroxyxenovulene B **4** and 4-dehydroxy

norpycnidione **5** significantly decreased EPO concentrations in hypomethylated FAIK3-5 cells. Thus, we found that the newly characterized 4-hydroxyxenovulene B **4** and 4-dehydroxy norpycnidione **5** compounds demonstrate versatile influences on cellular behaviour.

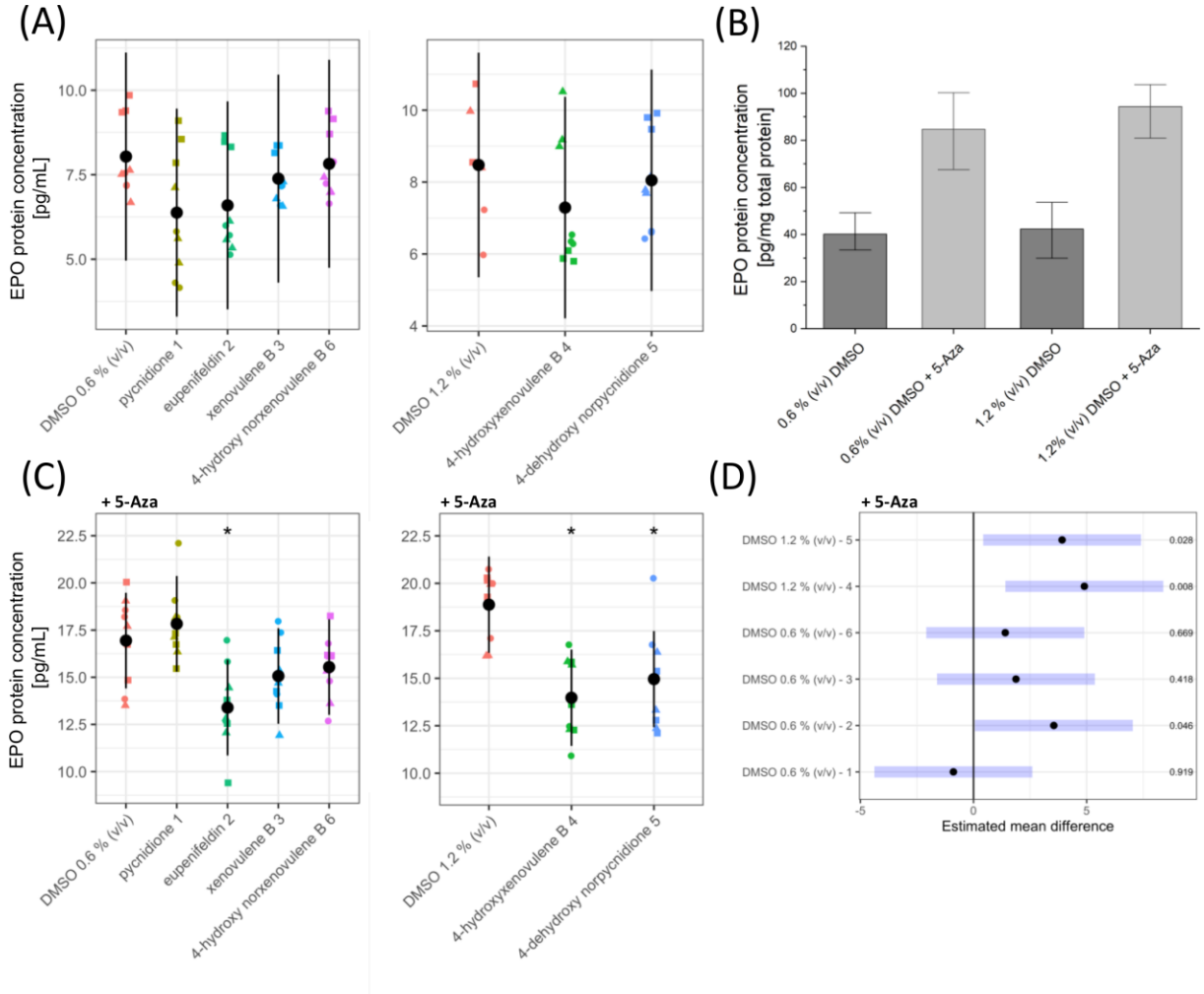

Fig. 5: Erythropoietin (EPO) content of FAIK3-5 samples treated with the tropolone sesquiterpenoids (TS) pycnidione **1**, eupenifeldin **2**, xenovulene B **3**, 4-hydroxyxenovulene B **4**, 4-dehydroxy norpycnidione **5** and tropolone-lacking compound 4-hydroxy norxenovulene B **6** and their respective vehicle controls (DMSO 0.6% (*v/v*), DMSO 1.2 % (*v/v*)). (A) EPO protein concentrations measured in three biological replicates (● = 1, ▲ = 2, ■ = 3) of FAIK3-5 cells treated with 6 µM of TS compounds **1**, **2**, **3**, tropolone- moiety lacking compound **6** and their respective DMSO vehicle control (0.6 % (*v/v*)) or 12 µM of TS compounds **4**, **5**, and their

respective DMSO vehicle control (1.2 % (v/v)) without pre-treatment of 5-Azacytidine (5-Aza). Block dots are indicating the model based least square means and their pointwise 95% confidence intervals (black bars). (B) Measurement of basic EPO protein content in FAIK3-5 DMSO vehicle controls (0.6 % (*v/v*) and 1.2 % (*v/v*) with and without 5-Aza treatment for 6 days. Error bars indicate the standard deviation of mean EPO concentrations. (C) EPO protein concentrations measured in three biological replicates (● = 1,▲ = 2, ■ = 3) of FAIK3-5 cells treated with 6 µM of TS compounds **1**, **2**, **3**, tropolone- moiety lacking compound **6** and their respective DMSO vehicle control (0.6% (*v/v*)), or 12 µM of TS compounds **4**, **5**, and their respective DMSO vehicle control (1.2% (v/v)) with pre-treatment of 5-Azacytidine (+ 5-Aza). Block dots are indicating the model based least square means and their pointwise 95% confidence intervals (black bars). Treatments marked with ***** are significantly different from their respective vehicle controls. (D) Pairwise mean comparisons showed significant differences in EPO protein concentrations 4-hydroxyxenovulene B **4**, 4-dehydroxy norpycnidione **5** and eupenifeldin **2** compared to their respective vehicle controls. Black dots indicate back transformed means of measured EPO concentrations and their 95% confidence intervals (blue bars). Respective p-values for each calculation are displayed on the right side. The estimated contrasts and corresponding confidence intervals are given in the Supporting Information S16.

4. Conclusion

In this study, we analyzed the influence of TS compound treatment on a murine REP derived cell line to find a link between their molecular structures and reported biological effects. We found that their bioactivity in terms of cytotoxicity and growth inhibition is strongly dependent on the tropolone proportions of the compounds used. Structurally, all monotropolones of the xenovulene-type exhibit an *E* configuration of the C-8 / C-9 alkene, which is also displayed in

xenovulene B **3** and 4-hydroxyxenovulene B **4**. However, as both compounds possess an intact tropolone nucleus, they are structurally related to the bioactive TS compounds pycnidione **1** and eupenifeldin **2.** We demonstrated that the two bistropolones pycnidione **1** and eupenifeldin **2** exhibited a significantly higher cytotoxic potency compared to the monotropolones xenovulene B **3** and 4-hydroxyxenovulene B **4**, for which these are the first bioactivities described in the literature, and, that monotropolones like xenovulene B **3** and 4-hydroxyxenovulene B **4,** or sesquiterpene phenols such as 4-dehydroxy norpycnidione **5** are significantly less potent or even unable to cause biological reactions in the tested cells. Our findings are substantiated by the earlier discovery that methylated pycnidione derivatives are inactive with respect to their described ability to induce EPO gene expression in hepatic cell lines [23] and their potential to enhance the effects of bleomycin treatment of Jurkat cells [19], and lead to the assumption that the number of unprotected tropolone moieties is essential for TS potency, although the exact structure-activity relationship of the compounds remains as-yet unclear.

The previous reports of EPO induction by TS compounds of the "epolone family" observed in the reporter cell lines Hep3B [23], HepG2, and HRCHO5 [24] led us to speculate that certain TS compounds might play a role in the induction of EPO synthesis independent of oxygen availability. We therefore hypothesized that tropolone-containing molecules might be able to mimic a hypoxic response in cells, e.g. by inhibiting proteins containing a HIF-prolyl hydroxylase domain, and that structurally related compounds might be able to trigger similar processes. Since the above-mentioned studies of epolone-induced EPO induction were previously performed on genetically modified hepatic cancer cell lines, we wanted to use a model that more closely matched physiological conditions. Therefore, we chose the nonconditionally immortalized murine REP-dervied cell line FAIK3-5 [36] as a model that can reflect natural EPO expression. In this study TS treatment showed no influence on EPO production on the REP derived FAIK3-5 cell line. However, because previous reports were

based on indirect measurements of EPO gene induction or performed on genetically engineered cancer cell lines, cell-type specific and transcriptional regulation of EPO expression may have been less accounted for and might be a reason for the contrasting results. Physiologically, EPO production is tightly regulated at the transcriptional level, whereas DNA methylation of the EPO promoter is partially involved in epigenetic inactivation of EPO expression [51]. This mechanism was also observed in the utilized REP cell line and the authors proposed the occurrence of an intrinsic transcriptional negative feedback loop responsible for the decline in EPO production upon longer cultivation periods [36]. Moreover, despite its universal use in cryopreservation or as a solvent for poorly soluble molecules, there is evidence of DMSO toxicity at low doses and its impacts on the epigenetic landscape of treated samples [50, 52], which may have further implications on protein expression after treatment. Correspondingly, also in this study we observed significant effects of DMSO on proliferation and cell viability, although the observed inhibition of cell growth and cytotoxicity were considerably lower than in samples treated with TS compound **1** – **5** or did not show a dose-response relationship.

To circumvent the effects of DNA methylation of the EPO-regulatory loci or the *Epo* locus itself, the cell line was treated with the DNA methyltransferase inhibitor 5-Aza for six days prior to TS compound treatment in a second approach. Indeed, we observed an increase in basic EPO production compared to samples with putative regulatory methylation under all conditions, yet, no significant enhancement after TS treatment compared to vehicle controls could be determined leading to the assumption that the complex "on-off" behavior of REP cells has a major impact on protein synthesis *in vitro*. Since EPO-producing cells are in a quiescent state *in vivo* [48], it is possible that this specific stage is required for normal oxygen sensing and signaling in cultured FAIK3-5 cells. Despite previous reports on the EPO enhancing influence of TS compounds like pycnidione **1**, in our study the addition of eupenifeldin **2**, 4-hydroxyxenuvolene B **4** or 4-dehydroxy norpycnidione **5** led to a significant decrease in basic EPO production in 5-Aza treated cells compared to vehicle controls, although we did not find

a direct correlation with the molecular structures of the compounds and the number of tropolone substitutions. Treatment with eupenifeldin **2** additionally resulted in significantly lower cell survival compared with untreated control samples, and cells treated with tropolone-lacking compound 4- hydroxyl norxenovulene B **6** and TS compound 4-dehydroxy norpycnidione **5,** which may explain the low protein concentration in these samples. Since we observed significant inhibition of proliferation by all studied tropolone-bearing TS compounds (**1**-**5**), the observed effects on cellular EPO content in 4-hydroxyxenuvolene B **4** or 4-dehydroxy norpycnidione **5** treated samples cannot be exclusively due to decreased total protein expression caused by low cellular metabolism.

In contrast to previous reports [23, 24], the measurement of EPO protein concentration in our study was not performed on genetically modified reporter cell lines and did not rely on indirect protein measurement methods such as firefly luciferase reporter assays. Despite their wide use in molecular biology and high-throughput screening assays for small molecules [53], firefly luciferase based assays can easily lead to biased signal output due to false-positive results caused by various types of assay interference. In particular, the counterintuitive phenomenon of signal activation by luciferase inhibitor molecules, in which inhibitors can prolong the half-life of the ectopically expressed luciferase enzyme, can lead to an increase in signal strength that is indistinguishable from transcriptional activation of the reporter gene [54]. These effects have already been reported for other bioactive compounds like sesquiterpene lactones, which inhibit luciferase activity probably by direct targeting of the enzyme [55] and have also been demonstrated on HepG2 cells stably expressing the luciferase enzyme [56]. Thompson et al. described that measured luciferase activities increased up to 20-fold in a concentration dependent manner after addition of potent luciferase inhibitors such PBT (Phenylbenzothiazole) or HPBT (2-hydroxyphenylbenzothiazole) to HepG2 cell culture medium. On the basis of these findings and in combination with the results of our study, it is very possible that the described EPO-enhancing properties of the reported epolone compounds

need to be reevaluated, and we emphasize the need for careful investigation of possible interference of the TS compounds with firefly luciferase-based drug screening assays.

Apart from their effect on protein expression, the treatment of TS compounds resulted in a strong inhibition of cell proliferation and morphological alteration in our model. The monotropolone compound 4-dehydroxy norpycnidione **5** showed a significantly improved proliferation inhibition compared to the tropolone-lacking compound 4-hydroxy norxenovulene B **6** and untreated control samples. However, at the same time cytotoxic effects exerted on the model cell line were significantly lower as those of pycnidione **1** or eupenifeldin **2**. The reduced toxicity and concomitant severe growth retardation induced by 4-dehydroxy norpycnidione **5** could be a sign of cell transition to a senescent stage.

In addition to cell growth discontinuation, alterations of cell morphology can also reflect senescent cell stages *in vitro* by the emergence of an enlarged, flat and multinucleated phenotype which is highly granulated [57]. In our study, we observed severe morphological alterations of FAIK3-5 cells treated with different TS compounds, although only 4-hydroxyxenovulene B **4** treated cells can partially live up to this description with the largest measured cell area compared to all other treatments, which is significantly increased ($p < 0.001$) compared to pycnidione **1** and 4-dehydroxy norpycnidione **5**. The occurrence of highly granulated cells, on the other hand, was visible in all treated samples. Apart from that, we observed that related chemical compounds such as pycnidione **1** and eupenifeldin **2**, as well as xenovulene B **3** and 4-hydroxyxenovulene B **4** induced similar phenotypic alteration in treated FAIK3-5 cells and assumed that the compounds most likely target similar biological pathways via specific receptors, thereby leading to same biological responses that are mirrored in cell morphology. In contrast to the mainly described morphological features related to cellular senescence, Brandhagen et al. observed that mifepristone-induced cytostasis in a panel of ovary cancer cell lines resulted in morphological changes, with cells developing a thin cytoplasm and neurite-like protrusions [58], similar to our observations of cells treated with both bistropolones

pycnidione **1** or eupenifeldin **2**. Brandhagen et al. provided evidence that senescence can also exhibit divergent phenotypes as usually described. Assuming that there are different types of senescence observed *in vitro* and induced by different stimuli (e.g. stress-induced, oncogene-induced or tumor surpressor loss-induced) [59], it is possible that some of the used TS compounds could have promoted senescence in FAIK3-5 samples despite the morphological differences between them. *In vitro* senescence is defined as irreversible loss proliferative potential of cells, thereby distinguishing it from reversible non-senescent growth arrest such as cellular quiescence, whereby overstimulation of initially quiescent cells can lead to physiological senescence. Due to their constant contact with serum containing cell culture medium, *in vitro* arrested cells can shift to senescence due to chronic over-stimulation with nutrients and growth factors [60]. Therefore, in this study, the exerted effect of TS compounds observable by significant proliferative inhibition can be the result of cell cycle arrest or senescence. However, considering that the bistropolone pycnidione **1** has already been described as inducing cell cycle arrest and, moreover, enhancing bleomycin cytotoxicity in Jurkat cells [19, 20], we might expect a similar mode of action of the related bioactive TS compounds, making them interesting targets for subsequent clinical studies.

This study thus provides first evidence of the bioactive properties of the analysed monotropolones xenovulene B **3**, 4-hydroxyxenovulene B **4** and 4-dehydroxy norpycnidione **5**. There is a significant relationship between the number of tropolone substitutions and cell viability. Moreover, eupenifeldin **2**, 4-hydroxyxenovulene B **4** and 4-dehydroxy norpycnidione **5** demonstrate versatile influences on cellular behaviour and reduce EPO content in hypomethylated FAIK3-5 cells. Compound **5** additionally exhibits significantly elevated proliferative inhibition paired with low cytotoxic effects on the tested cell line and might therefore serve as a putative compound for further pre-clinical drug testing studies for cancer treatment.

Acknowledgements

We would like to thank Frank Schaarschmidt for his valuable input and support in the biostatistics analysis of the experiments.

Funding

This work has been carried out within the framework of the SMART BIOTECS alliance between the Technische Universität Braunschweig and the Leibniz Universität Hannover. This initiative is supported by the Ministry of Science and Culture (MWK) of Lower Saxony, Germany. This project has also received funding from the European Research Council (ERC) under the European Union's Horizon 2020 research and innovation programme (grant agreement No 757490).

Conflict of Interest

The authors declare no conflict of interest.

Author Contributions

Timna Claire Bergmann: Investigation (lead), Methodology (lead), Formal Analysis (equal), Visualization (lead), Writing – original draft (lead). Max Menssen: Formal Analysis (lead), Visualization (equal), Writing – Review and Editing (equal). Carsten Schotte: Resources (lead), Writing – Review and Editing (equal). Russell J. Cox: Conceptualization (equal), Resources (equal), Writing – Review and Editing (equal). Cornelia Lee-Thedieck: Conceptualization (lead), Funding Acquisition (lead), Project Administration (lead), Supervision (lead), Writing – Review and Editing (lead)

Data Availability Statement

Additional data is available on request from the authors.

1 References

1 Peláez, F. (2005) Biological Activities of Fungal Metabolites, in *Handbook of industrial mycology* (ed Z. An), M. Dekker, New York, pp. 49–92.

2 Schueffler, A. and Anke, T. (2014) Fungal natural products in research and development. *Natural product reports*, **31** (10), 1425–1448.

3 Choy, K.W., Murugan, D., Mustafa, M.R. (2018) Natural products targeting ER stress pathway for the treatment of cardiovascular diseases. *Pharmacological research*, **132**, 119–129.

4 Langeder, J., Grienke, U., Chen, Y., Kirchmair, J., Schmidtke, M., Rollinger, J.M. (2020) Natural products against acute respiratory infections: Strategies and lessons learned. *Journal of Ethnopharmacology*, **248**, 112298.

5 Yu, S., Liu, M., Hu, K. (2019) Natural products: Potential therapeutic agents in multiple sclerosis. *International immunopharmacology*, **67**, 87–97.

6 Essa, M.M., Akbar, M., Guillemin, G. (2016) *The Benefits of Natural Products for Neurodegenerative Diseases*, Springer International Publishing; Imprint; Springer, Cham.

7 Demain, A.L. and Vaishnav, P. (2011) Natural products for cancer chemotherapy. *Microbial biotechnology*, **4** (6), 687–699.

8 Cragg, G.M., Grothaus, P.G., Newman, D.J. (2009) Impact of natural products on developing new anti-cancer agents. *Chemical reviews*, **109** (7), 3012–3043.

9 Abdelmohsen, U.R., Balasubramanian, S., Oelschlaeger, T.A., Grkovic, T., Pham, N.B., Quinn, R.J., Hentschel, U. (2017) Potential of marine natural products against drug-

resistant fungal, viral, and parasitic infections. *The Lancet Infectious Diseases*, **17** (2), e30-e41.

10 Hemaiswarya, S., Kruthiventi, A.K., Doble, M. (2008) Synergism between natural products and antibiotics against infectious diseases. *Phytomedicine : international journal of phytotherapy and phytopharmacology*, **15** (8), 639–652.

11 van Santen, J.A., Poynton, E.F., Iskakova, D., McMann, E., Alsup, T.A., Clark, T.N., Fergusson, C.H., Fewer, D.P., Hughes, A.H., McCadden, C.A., Parra, J., Soldatou, S., Rudolf, J.D., Janssen, E.M.-L., Duncan, K.R., Linington, R.G. (2022) The Natural Products Atlas 2.0: a database of microbially-derived natural products. *Nucleic acids research*, **50** (D1), D1317-D1323.

12 Harris, G.H., Hoogsteen, K., Silverman, K.C., Raghoobar, S.L., Bills, G.F., Lingham, R.B., Smith, J.L., Dougherty, H.W., Cascales, C., Peláez, F. (1993) Isolation and structure determination of pycnidione, A novel bistropolone stromelysin inhibitor from a Phoma sp. *Tetrahedron*, **49** (11), 2139–2144.

13 Mayerl, F., Gao, Q., Huang, S., Klohr, S.E., Matson, J.A., Gustavson, D.R., Pirnik, D.M., Berry, R.L., Fairchild, C., Rose, W.C. (1993) Eupenifeldin, a novel cytotoxic bistropolone from Eupenicillium brefeldianum. *J. Antibiot.*, **46** (7), 1082–1088.

14 Li, L. and Cox, R.J. (2022) Stereochemical and Biosynthetic Rationalisation of the Tropolone Sesquiterpenoids. *Journal of fungi (Basel, Switzerland)*, **8** (9).

15 Bemis, C.Y., Ungarean, C.N., Shved, A.S., Jamieson, C.S., Hwang, T., Lee, K.S., Houk, K.N., Sarlah, D. (2021) Total Synthesis and Computational Investigations of Sesquiterpene-Tropolones Ameliorate Stereochemical Inconsistencies and Resolve an Ambiguous Biosynthetic Relationship. *Journal of the American Chemical Society*, **143** (15), 6006–6017.

16 Bunyapaiboonsri, T., Veeranondha, S., Boonruangprapa, T., Somrithipol, S. (2008) Ramiferin, a bisphenol-sesquiterpene from the fungus Kionochaeta ramifera BCC 7585. *Phytochemistry Letters*, **1** (4), 204–206.

17 Al Subeh, Z.Y., Chu, N.-Q., Korunes-Miller, J.T., Tsai, L.L., Graf, T.N., Hung, Y.P., Pearce, C.J., Grinstaff, M.W., Colby, A.H., Colson, Y.L., Oberlies, N.H. (2021) Delivery of eupenifeldin via polymer-coated surgical buttresses prevents local lung cancer recurrence. *Journal of controlled release : official journal of the Controlled Release Society*, **331**, 260–269.

18 Pittayakhajonwut, P., Theerasilp, M., Kongsaeree, P., Rungrod, A., Tanticharoen, M., Thebtaranonth, Y. (2002) Pughiinin A, a Sesquiterpene from the Fungus Kionochaeta pughii BCC 3878. *Planta Med*, **68** (11), 1017–1019.

19 Kaneko, M., Matsuda, D., Ohtawa, M., Fukuda, T., Nagamitsu, T., Yamori, T., Tomoda, H. (2012) Potentiation of bleomycin in Jurkat cells by fungal pycnidione. *Biological & pharmaceutical bulletin*, **35** (1), 18–28.

20 Hsiao, C.-J., Hsiao, S.-H., Chen, W.-L., Guh, J.-H., Hsiao, G., Chan, Y.-J., Lee, T.-H., Chung, C.-L. (2012) Pycnidione, a fungus-derived agent, induces cell cycle arrest and apoptosis in A549 human lung cancer cells. *Chemico-biological interactions*, **197** (1), 23–30.

21 Höller, U., Wright, A.D., Matthee, G.F., Konig, G.M., Draeger, S., Aust, H.-J., Schulz, B. (2000) Fungi from marine sponges: diversity, biological activity and secondary metabolites. *Mycological Research*, **104** (11), 1354–1365.

22 Wright, A.D. and Lang-Unnasch, N. (2005) Potential antimalarial lead structures from fungi of marine origin. *Planta medica*, **71** (10), 964–966.

23 Cai, P., Smith, D., Cunningham, B., Brown-Shimer, S., Katz, B., Pearce, C., Venables, D., Houck, D. (1998) Epolones: novel sesquiterpene-tropolones from fungus OS-F69284 that induce erythropoietin in human cells. *Journal of natural products*, **61** (6), 791–795.

24 Wanner, R.M., Spielmann, P., Stroka, D.M., Camenisch, G., Camenisch, I., Scheid, A., Houck, D.R., Bauer, C., Gassmann, M., Wenger, R.H. (2000) Epolones induce erythropoietin expression via hypoxia-inducible factor-1 alpha activation. *Blood*, **96** (4), 1558–1565.

25 Chen, S., Liu, Z., Tan, H., Chen, Y., Li, S., Li, H., Zhu, S., Liu, H., Zhang, W. (2020) Phomeroids A and B: two novel cytotoxic meroterpenoids from the deep-sea-derived fungus Phomopsis tersa FS441. *Org. Chem. Front.*, **7** (3), 557–562.

26 El-Elimat, T., Raja, H.A., Ayers, S., Kurina, S.J., Burdette, J.E., Mattes, Z., Sabatelle, R., Bacon, J.W., Colby, A.H., Grinstaff, M.W., Pearce, C.J., Oberlies, N.H. (2019) Meroterpenoids from Neosetophoma sp.: A Dioxa4.3.3propellane Ring System, Potent Cytotoxicity, and Prolific Expression. *Organic letters*, **21** (2), 529–534.

27 Bunyapaiboonsri, T., Veeranondha, S., Boonruangprapa, T., Somrithipol, S. (2008) [Copy] Ramiferin, a bisphenol-sesquiterpene from the fungus Kionochaeta ramifera BCC 7585. *Phytochemistry Letters*, **1** (4), 204–206.

28 Pittayakhajonwut, P., Theerasilp, M., Kongsaeree, P., Rungrod, A., Tanticharoen, M., Thebtaranonth, Y. (2002) [Copy] Pughiinin A, a Sesquiterpene from the Fungus Kionochaeta pughii BCC 3878. *Planta Med*, **68** (11), 1017–1019.

29 Ainsworth, A.M., Chicarelli-Robinson, M.I., Copp, B.R., Fauth, U., Hylands, P.J., Holloway, J.A., Latif, M., O'Beirne, G.B., Porter, N., Renno, D.V. (1995) Xenovulene A, a novel GABA-benzodiazepine receptor binding compound produced by Acremonium strictum. *The Journal of Antibiotics*, **48** (7), 568–573.

30 Raggatt, M.E., Simpson, T.J., Inês Chicarelli-Robinson, M. (1997) Biosynthesis of Xenovulene A®: formation of a cyclopentenone via a unique ring expansion–ring contraction mechanism. *Chem. Commun.* (22), 2245–2247.

31 Schor, R., Schotte, C., Wibberg, D., Kalinowski, J., Cox, R.J. (2018) Three previously unrecognised classes of biosynthetic enzymes revealed during the production of xenovulene A. *Nat Commun*, **9** (1), 1963.

32 Schotte, C., Li, L., Wibberg, D., Kalinowski, J., Cox, R.J. (2020) Synthetic Biology Driven Biosynthesis of Unnatural Tropolone Sesquiterpenoids. *Angewandte Chemie (International ed. in English)*, **59** (52), 23870–23878.

33 Rokas, A., Mead, M.E., Steenwyk, J.L., Raja, H.A., Oberlies, N.H. (2020) Biosynthetic gene clusters and the evolution of fungal chemodiversity. *Natural product reports*, **37** (7), 868–878.

34 Yang, Z.-Y., He, J.-H., Lu, A.-P., Hou, T.-J., Cao, D.-S. (2020) Frequent hitters: nuisance artifacts in high-throughput screening. *Drug discovery today*, **25** (4), 657–667.

35 Obara, N., Suzuki, N., Kim, K., Nagasawa, T., Imagawa, S., Yamamoto, M. (2008) Repression via the GATA box is essential for tissue-specific erythropoietin gene expression. *Blood*, **111** (10), 5223–5232.

36 Imeri, F., Nolan, K.A., Bapst, A.M., Santambrogio, S., Abreu-Rodríguez, I., Spielmann, P., Pfundstein, S., Libertini, S., Crowther, L., Orlando, I.M.C., Dahl, S.L., Keodara, A., Kuo, W., Kurtcuoglu, V., Scholz, C.C., Qi, W., Hummler, E., Hoogewijs, D., Wenger, R.H. (2019) Generation of renal Epo-producing cell lines by conditional gene tagging reveals rapid HIF-2 driven Epo kinetics, cell autonomous feedback regulation, and a telocyte phenotype. *Kidney international*, **95** (2), 375–387.

37 Ziegler, S., Sievers, S., Waldmann, H. (2021) Morphological profiling of small molecules. *Cell chemical biology*, **28** (3), 300–319.

38 Xiong, Y. and Iglesias, P.A. (2010) Tools for analyzing cell shape changes during chemotaxis. *Integrative biology : quantitative biosciences from nano to macro*, **2** (11-12), 561–567.

39 Chen, C.S., Mrksich, M., Huang, S., Whitesides, G.M., Ingber, D.E. (1997) Geometric control of cell life and death. *Science (New York, N.Y.)*, **276** (5317), 1425–1428.

40 Watson, P.A. (1991) Function follows form: generation of intracellular signals by cell deformation. *FASEB journal : official publication of the Federation of American Societies for Experimental Biology*, **5** (7), 2013–2019.

41 Lobo, J., See, E.Y.-S., Biggs, M., Pandit, A. (2016) An insight into morphometric descriptors of cell shape that pertain to regenerative medicine. *Journal of tissue engineering and regenerative medicine*, **10** (7), 539–553.

42 Arganda-Carreras, I., Fernández-González, R., Muñoz-Barrutia, A., Ortiz-De-Solorzano, C. (2010) 3D reconstruction of histological sections: Application to mammary gland tissue. *Microscopy research and technique*, **73** (11), 1019–1029.

43 Heisler, J., Elvir, L., Barnouti, F., Charles, E., Wolkow, T.D., Pyati, R. (2014) Morphological Effects of Natural Products on Schizosaccharomyces pombe Measured by Imaging Flow Cytometry. *Natural products and bioprospecting*, **4** (1), 27–35.

44 Sailem, H.Z., Sero, J.E., Bakal, C. (2015) Visualizing cellular imaging data using PhenoPlot. *Nat Commun*, **6** (1), 5825.

45 Doncel, J.P., La Ojeda, P.d.C., OropesaÁvila, M., Paz, M.V., Lavera, I. de, La Mata, M.D., Córdoba, M.Á., Hidalgo, R.L., Rivero, J.M.S., Cotán, D., Sánchez‐Alcázar, J.A. (2017) Cytoskeleton Rearrangements during the Execution Phase of Apoptosis, in *Cytoskeleton - Structure, Dynamics, Function and Disease* (ed J.C. Jimenez-Lopez), IntechOpen, Erscheinungsort nicht ermittelbar.

46 Farshori, N.N., Siddiqui, M.A., Al-Oqail, M.M., Al-Sheddi, E.S., Al-Massarani, S.M., Saquib, Q., Ahmad, J., Al-Khedhairy, A.A. (2022) Aloe vera-induced apoptotic cell death through ROS generation, cell cycle arrest, and DNA damage in human breast cancer cells. *Biologia*.

47 Dahl, S.L., Pfundstein, S., Hunkeler, R., Dong, X., Knöpfel, T., Spielmann, P., Scholz, C.C., Nolan, K.A., Wenger, R.H. (2022) Fate-mapping of erythropoietin-producing cells in mouse models of hypoxaemia and renal tissue remodelling reveals repeated recruitment and persistent functionality. *Acta Physiologica (Oxford, England)*, **234** (3), e13768.

48 Souma, T., Yamazaki, S., Moriguchi, T., Suzuki, N., Hirano, I., Pan, X., Minegishi, N., Abe, M., Kiyomoto, H., Ito, S., Yamamoto, M. (2013) Plasticity of renal erythropoietin-producing cells governs fibrosis. *Journal of the American Society of Nephrology : JASN*, **24** (10), 1599–1616.

49 Chang, Y.-T., Yang, C.-C., Pan, S.-Y., Chou, Y.-H., Chang, F.-C., Lai, C.-F., Tsai, M.-H., Hsu, H.-L., Lin, C.-H., Chiang, W.-C., Wu, M.-S., Chu, T.-S., Chen, Y.-M., Lin, S.-L. (2016) DNA methyltransferase inhibition restores erythropoietin production in fibrotic murine kidneys. *The Journal of clinical investigation*, **126** (2), 721–731.

50 Verheijen, M., Lienhard, M., Schrooders, Y., Clayton, O., Nudischer, R., Boerno, S., Timmermann, B., Selevsek, N., Schlapbach, R., Gmuender, H., Gotta, S., Geraedts, J., Herwig, R., Kleinjans, J., Caiment, F. (2019) DMSO induces drastic changes in human cellular processes and epigenetic landscape in vitro. *Scientific reports*, **9** (1), 4641.

51 Sato, K., Hirano, I., Sekine, H., Miyauchi, K., Nakai, T., Kato, K., Ito, S., Yamamoto, M., Suzuki, N. (2019) An immortalized cell line derived from renal erythropoietin-producing (REP) cells demonstrates their potential to transform into myofibroblasts. *Scientific reports*, **9** (1), 11254.

52 Galvao, J., Davis, B., Tilley, M., Normando, E., Duchen, M.R., Cordeiro, M.F. (2014) Unexpected low-dose toxicity of the universal solvent DMSO. *FASEB journal : official publication of the Federation of American Societies for Experimental Biology*, **28** (3), 1317–1330.

53 Thorne, N., Inglese, J., Auld, D.S. (2010) Illuminating insights into firefly luciferase and other bioluminescent reporters used in chemical biology. *Chemistry & biology*, **17** (6), 646–657.

54 Auld, D.S., Thorne, N., Nguyen, D.-T., Inglese, J. (2008) A specific mechanism for nonspecific activation in reporter-gene assays. *ACS chemical biology*, **3** (8), 463–470.

55 Lindenmeyer, M.T., García-Piñeres, A.J., Castro, V., Merfort, I. (2004) Sesquiterpene lactones inhibit luciferase but not beta-galactosidase activity in vitro and ex vivo. *Analytical Biochemistry*, **328** (2), 147–154.

56 Thompson, J.F., Hayes, L.S., Lloyd, D.B. (1991) Modulation of firefly luciferase stability and impact on studies of gene regulation. *Gene*, **103** (2), 171–177.

57 Beck, J., Horikawa, I., Harris, C. (2020) Cellular Senescence: Mechanisms, Morphology, and Mouse Models. *Veterinary pathology*, **57** (6), 747–757.

58 Brandhagen, B.N., Tieszen, C.R., Ulmer, T.M., Tracy, M.S., Goyeneche, A.A., Telleria, C.M. (2013) Cytostasis and morphological changes induced by mifepristone in human metastatic cancer cells involve cytoskeletal filamentous actin reorganization and impairment of cell adhesion dynamics. *BMC cancer*, **13**, 35.

59 Kuilman, T., Michaloglou, C., Mooi, W.J., Peeper, D.S. (2010) The essence of senescence. *Genes & development*, **24** (22), 2463–2479.

60 Blagosklonny, M.V. (2011) Cell cycle arrest is not senescence. *Aging*, **3** (2), 94–101.

61 Schindelin, J., Arganda-Carreras, I., Frise, E., Kaynig, V., Longair, M., Pietzsch, T., Preibisch, S., Rueden, C., Saalfeld, S., Schmid, B., Tinevez, J.-Y., White, D.J., Hartenstein, V., Eliceiri, K., Tomancak, P., Cardona, A. (2012) Fiji: an open-source platform for biological-image analysis. *Nature methods*, **9** (7), 676–682.

Supporting Information

Bioactive effects of natural and novel unnatural tropolone sesquiterpenoids in a murine cell model of renal interstitial fibroblasts

Timna Claire Bergmann, Max Menssen, Carsten Schotte, Russell J. Cox, Cornelia Lee-Thedieck

T.C. Bergmann, Prof. Dr. C. Lee-Thedieck

Institute of Cell Biology and Biophysics, Department of Cell Biology, Leibniz University Hannover, 30419 Hannover, Germany

Corresponding Author E-mail: lee-thedieck@cell.uni-hannover.de

Dr. M. Menssen

Institute of Cell Biology and Biophysics, Department of Biostatistics, Leibniz University Hannover, 30419 Hannover, Germany

Dr. C. Schotte, Prof. Dr. R.J.Cox

Institute of Organic Chemistry and BMWZ, Leibniz University Hannover, 30167 Hannover, Germany

Keywords: tropolone sesquiterpenoids, synthetic biology, bioactivity, proliferation, cytotoxicity, erythropoietin

Fig. S1. Workflow for analysis of morphometric parameters and ramification patterns. (A) Original image with selected regions of interest (ROIs). ROIs were drawn by hand to ensure the most accurate depiction of cell shapes and calculation of area, standard deviation, minimal and maximal grey value, mean grey value, shape descriptors (aspect ratio, circularity, roundness and solidity), perimeter and fit ellipse was conducted in Fiji (ImageJ Version 1.53c bundled with Java 1.8.0_172) [1] and used for visualization via PhenoPlot software [2]. (B) For the analysis of ramification patterns, selected ROIs of separated cellular shapes were used to create a binary image, on which (C) the "Skeletonize 2D/3D" and "Analyze Skeleton (2D/3D)" [3] plugins were used for visualization and calculation of e.g. branch numbers (via connection of end-points, end-points and junctions, or junctions and junctions), number of branch junctions, average and maximum length of branches. The obtained values for geometrical features, shape descriptors and branch numbers were normalized to the highest obtained mean value of each analysed parameter for subsequent visualization in PhenoPlot.

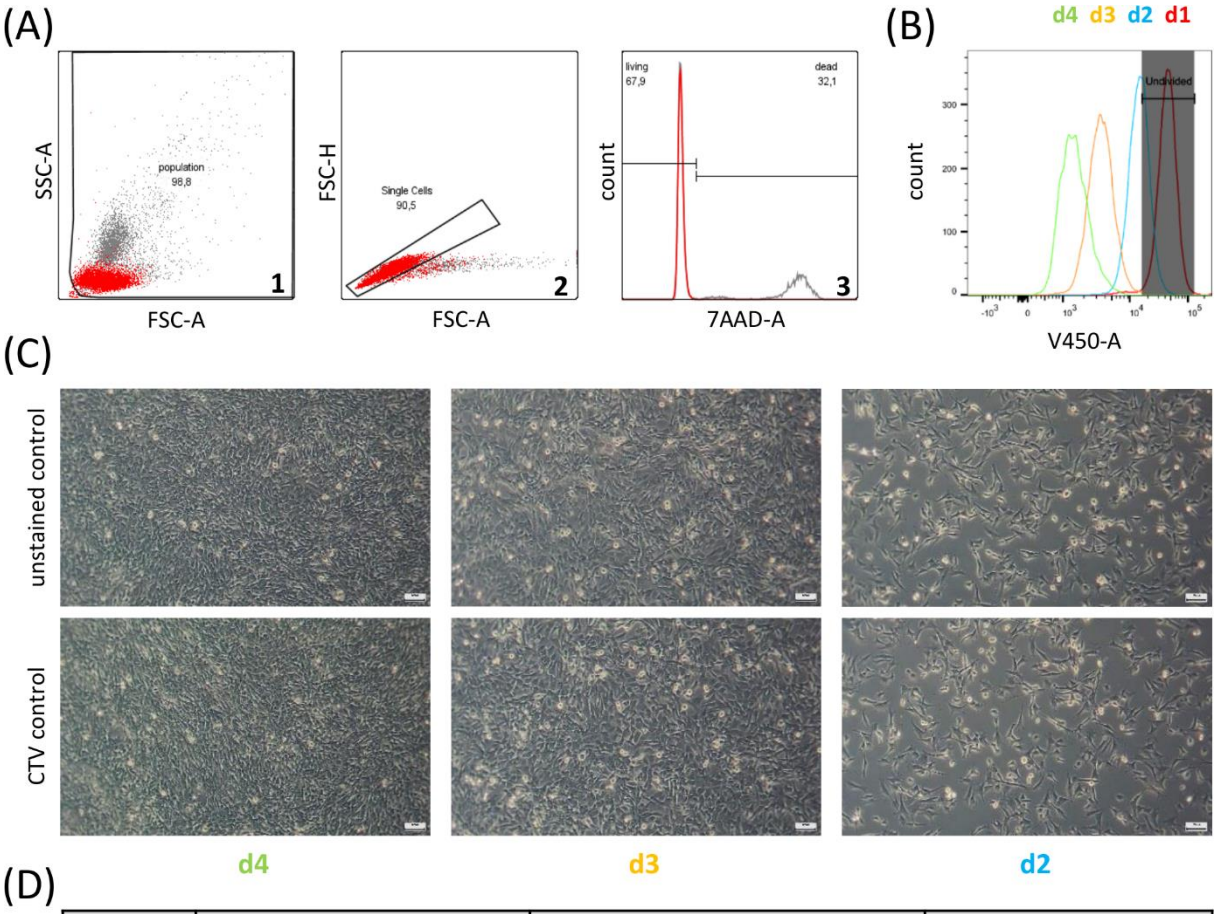

(D)

	mean fluorescence intensity	counted living cells	viability [%]
d1	46147	8393	91.7
d2	15444	9535	97.0
d3	3936	9432	97.4
d4	1693	9482	98.3

Fig. S2. Gating strategy for cytotoxicity assessment and proliferation analysis and preliminary tests on FAIK3-5 cells to assess optimal experimental conditions for subsequent proliferation analysis. (A) Backgating plots of the living cell population show the strategy for living/dead discrimination in a living/dead control sample comprising 50 % of heat-killed FAIK3-5 cells. After out-gating of (1) cell debris and (2) doublets, the (3) living and dead population is visualized in a histogram showing fluorescence intensities of Sytox AADvanced stained cells (7AAD-A channel). Thereafter, the threshold for dead cells' fluorescence intensities was set in the living/dead control and assigned to the remaining samples. (B) For proliferation analysis the mean fluorescence intensity (MFI) of cell trace violet (CTV, measured in V450-A channel)

of samples on d1 was set as undivided population in the living cell population of the analysed samples. To assess the optimal staining period for proliferation tests, CTV intensities and cell viability of stained FAIK3-5 cells were analysed on three subsequent days. (C, D) Proliferative behavior of FAIK3-5 cells was evaluated by normalizing the measured fluorescence intensities at day 2 - 4 to their respective MFIs of the undivided population at d1 of the experiment. As the cells continuously proliferate (C), the intensity of CTV decreases with each cell division, while cell viability remains over 90 % (D). For CTV staining and living/dead analysis 10 000 events per sample were counted.

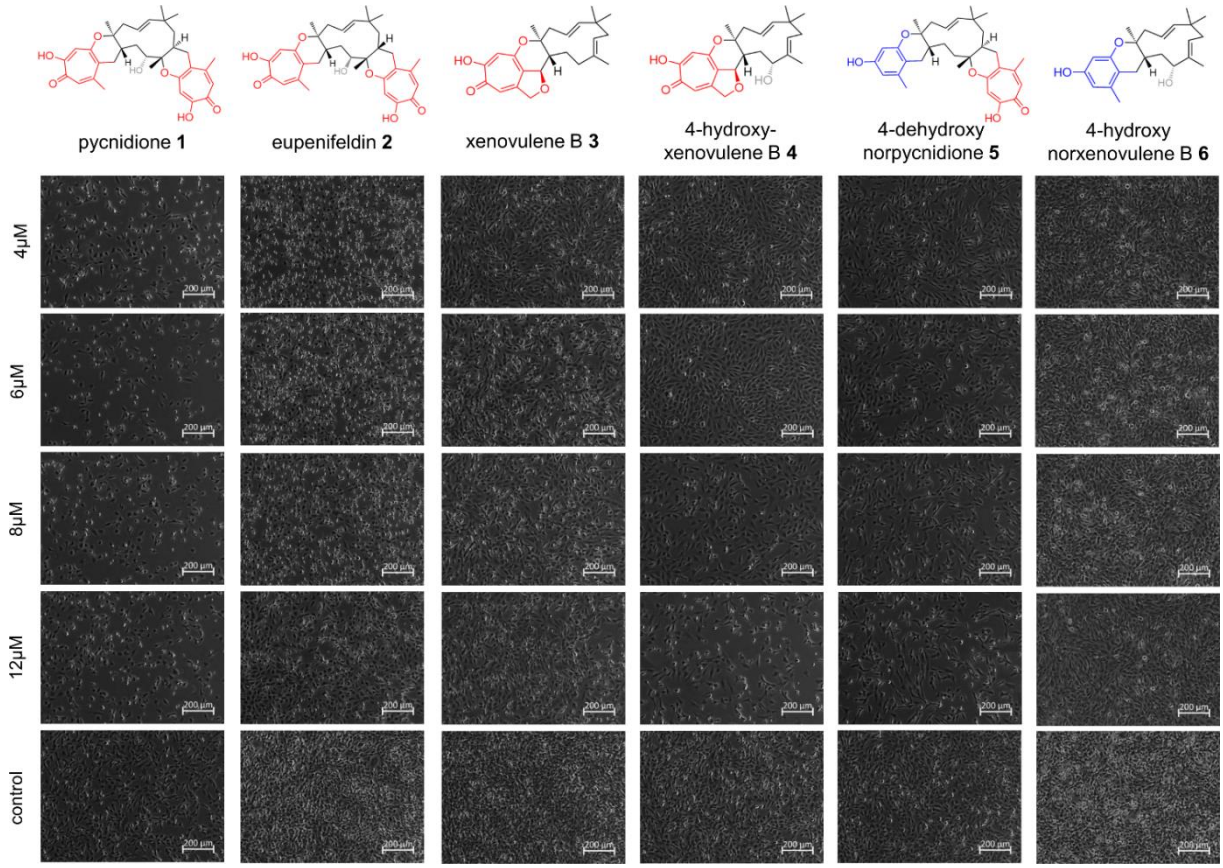

Fig. S3. Phase contrast images of FAIK3-5 cell samples treated with 4 µM, 6 µM, 8 µM, and 12 µM of tropolone-sesquiterpenoids (TS) (pycnidione **1**, eupenifeldin **2**, xenovulene B **3**, 4-hydroxyxenovulene B **4** and 4-dehydroxy norpycnidione **5**), TS moiety-lacking compound 4-hydroxy norxenovulene B **6** or cell culture medium (control) for 24 h. Structural formulae show highlighted key features of analyzed compounds in red (= polyketide derived tropolones), blue (= benzopyranyl moiety) and grey (C-10 hydroxylation).

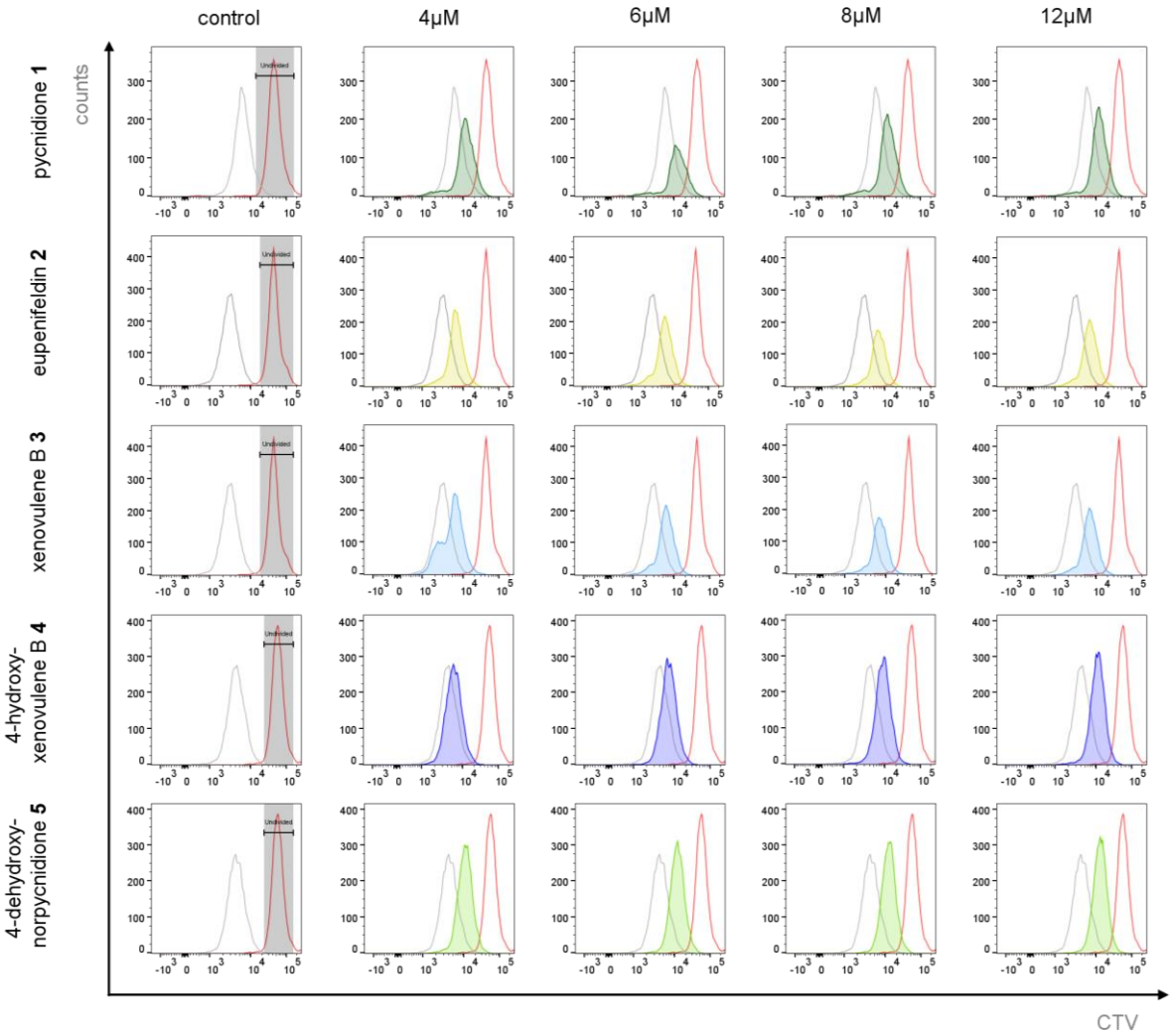

Fig. S4. Proliferation decrease of FAIK3-5 cells treated with 4 µM, 6 µM, 8 µM and 12 µM of tropolone-sesquiterpenoids (TS) (pycnidione **1**, eupenifeldin **2**, xenovulene B **3**, 4-hydroxyxenovulene B **4** and 4-dehydroxy norpycnidione **5**) for 24 h. Cell trace violet (CTV) stained cells were measured in a flow cytometer directly after staining to evaluate mean fluorescence intensities (MFI) of the undivided population (red) and 24 h after TS-compound treatment. MFI plots indicate a dose-independent decrease of proliferation in samples treated with pycnidione **1** (dark green), eupenifeldin **2** (yellow), xenovulene B **3** (light blue) and 4-dehydroxy norpycnidione **5** (light green), and a dose-dependent growth deceleration in 4-

hydroxyxenovulene B **4** (dark blue) treated samples assessed by consistently or increasingly higher MFI values compared to untreated controls (grey).

Table S5. Mean fluorescence (MFI) values, growth deceleration rates and cell viability of FAIK3-5 cells treated with tropolone sesquiterpenoids (TS) (pycnidione **1**, eupenifeldin **2**, xenovulene B **3**, 4-hydroxyxenovulene B **4** and 4-dehydroxy norpycnidione **5**), tropolone moiety lacking compound 4-hydroxy norxenovulene B **6** (N=3) and DMSO vehicle controls (N=3) in a concentration rage of 0 µM, 4 µM, 6 µM, 8 µM and 12 µM or respective volume percentages (0 % (v/v), 0.4 % (v/V), 0.6 % (v/v), 0.8 % (v/v) and 1.2 % (v/v). MFI values of cell trace violet stained samples indicate proliferative behaviour of cell samples, whereby higher intensities imply a downshift of cell divisions. Measurements were conducted 24 h after compound treatment and fold changes as well as percentages of growth deceleration were calculated with respect to untreated control samples (0 µM and 0 % (v/v)). Thereby, positive percentages demonstrate decreased cell proliferation compared to the untreated control sample and vice versa. Percentages of cell viability were obtained via SYTOX™ AADvanced™ staining and subsequent flow cytometric analysis.

	MFI (a.u.)					fold change			
	0µM	*4µM*	*6µM*	*8µM*	*12µM*	*4µM*	*6µM*	*8µM*	*12µM*
pycnidione **1**	7124	12485	13732	12962	12985	1.75	1.93	1.82	1.82
eupenifeldin **2**	2946	6390	6689	6573	6747	2.17	2.27	2.23	2.29
xenovulene B **3**	3340	6937	6689	7281	7397	2.08	2.00	2.18	2.21
4-hydroxyxenovulene B **4**	4108	5664	6792	8736	10747	1.38	1.65	2.13	2.62
4-dehydroxy norpycnidione **5**	4091	10530	11534	12018	12496	2.57	2.82	2.94	3.05
4-hydroxy norxenovulene B **6** (1)	2723	2739	2804	2761	2849	1.01	1.03	1.01	1.05
4-hydroxy norxenovulene B **6** (2)	4066	4041	4185	4211	4334	0.99	1.03	1.04	1.07
4-hydroxy norxenovulene B **6** (3)	3808	3823	3870	4180	4254	1.00	1.02	1.10	1.12
	0% (v/v)	*0.4% (v/v)*	*0.6% (v/v)*	*0.8% (v/v)*	*1.2% (v/v)*	*0.4% (v/v)*	*0.6% (v/v)*	*0.8% (v/v)*	*1.2% (v/v)*
DMSO (1)	2697	2697	2755	2676	2888	1.00	1.02	0.99	1.07
DMSO (2)	4066	3983	3999	4066	4308	0.98	0.98	1.00	1.06
DMSO (3)	3808	3967	3942	4099	4299	1.04	1.04	1.08	1.13

	growth deceleration compared to untreated control [%]			
	4µM	*6µM*	*8µM*	*12µM*
pycnidione **1**	75.25	92.75	81.95	82.27
eupenifeldin **2**	116.90	127.05	123.12	129.02
xenovulene B **3**	107.69	100.27	117.99	121.47
4-hydroxyxenovulene B **4**	37.88	65.34	112.66	161.61
4-dehydroxy norpycnidione **5**	157.39	181.94	193.77	205.45
4-hydroxy norxenovulene B **6** (1)	0.59	2.97	1.40	4.63
4-hydroxy norxenovulene B **6** (2)	-0.61	2.93	3.57	6.59
4-hydroxy norxenovulene B **6** (3)	0.39	1.63	9.77	11.71
	0.4% (v/v)	*0.6% (v/v)*	*0.8% (v/v)*	*1.2% (v/v)*
DMSO (1)	0.00	2.15	-0.78	7.08
DMSO (2)	-2.04	-1.65	0.00	5.95
DMSO (3)	4.18	3.52	7.64	12.89

	cell viability [%]				
	0µM	*4µM*	*6µM*	*8µM*	*12µM*
pycnidione **1**	91.9	68.9	48.5	71.1	71.8
eupenifeldin **2**	99.9	72.1	69.4	55.8	66.8
xenovulene B **3**	99.8	91.7	92.0	88.6	88.7
4-hydroxyxenovulene B **4**	99.9	96.4	96.1	95.7	94.4
4-dehydroxy norpycnidione **5**	99.9	95.4	93.4	95.0	95.9
4-hydroxy norxenovulene B **6** (1)	99.8	93.0	98.5	96.4	94.4
4-hydroxy norxenovulene B **6** (2)	98.9	98.8	98.2	98.9	98.2
4-hydroxy norxenovulene B **6** (3)	99.7	95.8	97.4	97.3	96.6
	0% (v/v)	*0.4% (v/v)*	*0.6% (v/v)*	*0.8% (v/v)*	*1.2% (v/v)*
DMSO (1)	99.8	97.7	91.7	97.8	97.6
DMSO (2)	99.8	98.6	98.7	99.0	97.8
DMSO (3)	99.7	97.5	96.6	98.4	95.0

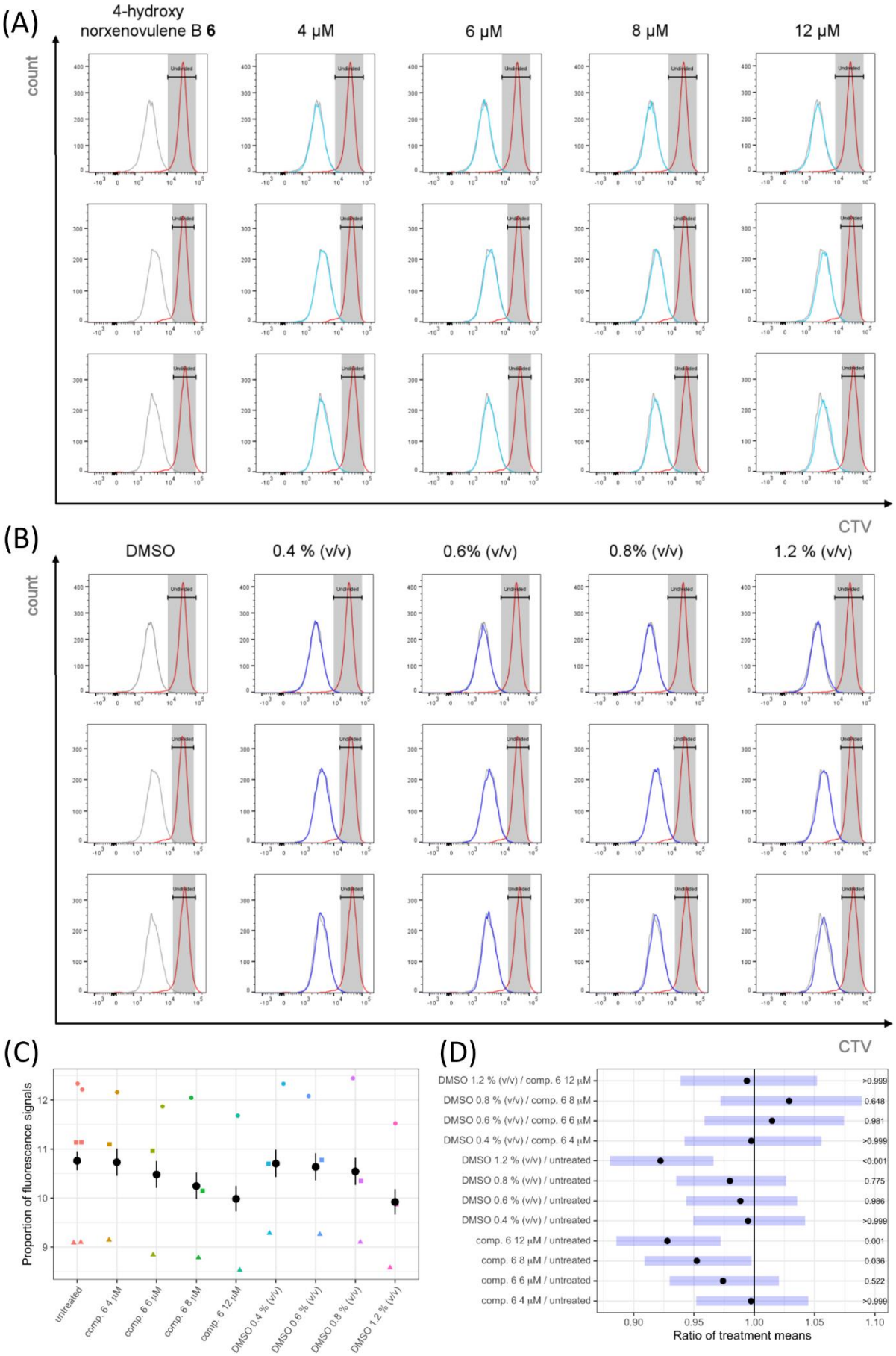
(A)
4-hydroxy norxenovulene B 6
4 µM
6 µM
8 µM
12 µM
count
CTV
(B)
DMSO
0.4 % (v/v)
0.6% (v/v)
0.8% (v/v)
1.2 % (v/v)
count
CTV
(C)
Proportion of fluorescence signals
untreated
comp. 6 4 µM
comp. 6 6 µM
comp. 6 8 µM
comp. 6 12 µM
DMSO 0.4 % (v/v)
DMSO 0.6 % (v/v)
DMSO 0.8 % (v/v)
DMSO 1.2 % (v/v)
(D)
DMSO 1.2 % (v/v) / comp. 6 12 µM >0.999
DMSO 0.8 % (v/v) / comp. 6 8 µM 0.648
DMSO 0.6 % (v/v) / comp. 6 6 µM 0.981
DMSO 0.4 % (v/v) / comp. 6 4 µM >0.999
DMSO 1.2 % (v/v) / untreated <0.001
DMSO 0.8 % (v/v) / untreated 0.775
DMSO 0.6 % (v/v) / untreated 0.986
DMSO 0.4 % (v/v) / untreated >0.999
comp. 6 12 µM / untreated 0.001
comp. 6 8 µM / untreated 0.036
comp. 6 6 µM / untreated 0.522
comp. 6 4 µM / untreated >0.999
Ratio of treatment means

Fig. S6. Proliferation decrease of FAIK3-5 cells treated with the tropolone-lacking compound 4-hydroxy norxenovulene B **6** and respective concentrations of the vehicle control DMSO for 24 h. (A, B) Cell trace violet (CTV) stained cells were measured in a flow cytometer directly after staining to evaluate mean fluorescence intensities (MFI) of the undivided population (red) and 24 h after incubation with 4 µM, 6 µM, 8 µM and 12 µM of 4-hydroxy norxenovulene B **6** (light blue), 0.4% (v/v), 0.6% (v/v), 0.8% (v/v) and 1.2% (v/v) of the DMSO vehicle control (dark blue) and untreated controls (grey). (C) For statistical analysis obtained MFI values were normalized by calculating the proportions of measured fluorescence signals on d1 and d3. The graphic shows the observed proportions of fluorescence signals (y^1/y^3) for each treatment and their corresponding least square means (black dots) together with 95% confidence intervals. (D) Pairwise mean comparisons between 4-hydroxy norxenovulene, DMSO and the untreated control. The black line indicates the null hypothesis that the ratio between the average fluorescence signals (black dots) is one. The blue horizontal bars indicate simultaneous 95 % confidence intervals for the mean ratios. If a confidence interval encompasses the one, the ratio does not significantly differ from one. The numbers on the right side of the graphic are the p-values of the corresponding test (see Supporting Information S11).

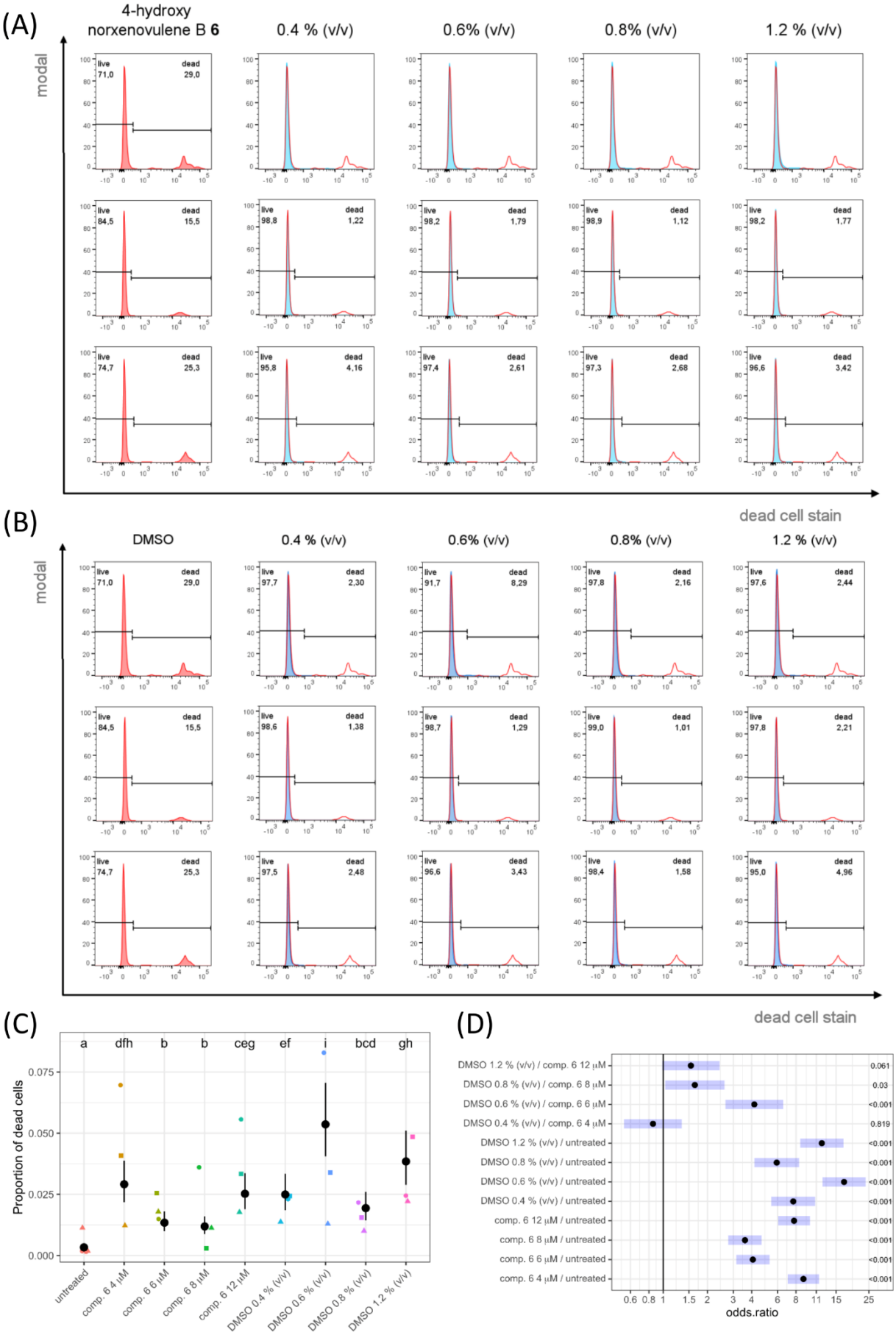
(A)
4-hydroxy norxenovulene B 6
0.4 % (v/v)
0.6% (v/v)
0.8% (v/v)
1.2 % (v/v)
modal
dead cell stain
(B)
DMSO
0.4 % (v/v)
0.6% (v/v)
0.8% (v/v)
1.2 % (v/v)
modal
dead cell stain
(C)
a
dfh
b
b
ceg
ef
i
bcd
gh
Proportion of dead cells
untreated
comp. 6 4 µM
comp. 6 6 µM
comp. 6 8 µM
comp. 6 12 µM
DMSO 0.4 % (v/v)
DMSO 0.6 % (v/v)
DMSO 0.8 % (v/v)
DMSO 1.2 % (v/v)
(D)
DMSO 1.2 % (v/v) / comp. 6 12 µM
DMSO 0.8 % (v/v) / comp. 6 8 µM
DMSO 0.6 % (v/v) / comp. 6 6 µM
DMSO 0.4 % (v/v) / comp. 6 4 µM
DMSO 1.2 % (v/v) / untreated
DMSO 0.8 % (v/v) / untreated
DMSO 0.6 % (v/v) / untreated
DMSO 0.4 % (v/v) / untreated
comp. 6 12 µM / untreated
comp. 6 8 µM / untreated
comp. 6 6 µM / untreated
comp. 6 4 µM / untreated
odds.ratio

Fig. S7. Assessment of cell viability of FAIK3-5 cells treated with (A) the tropolone moiety lacking compound 4-hydroxy norxenovulene B 6 and (B) DMSO vehicle control in a concentration rage of 0 µM, 4 µM, 6 µM, 8 µM and 12 µM or respective volume percentages (0 % (v/v), 0.4 % (v/v), 0.6 % (v/v), 0.8 % (v/v) and 1.2 % (v/v). Percentages of dead cells were obtained via SYTOX™ AADvanced™ dead cell staining and flow cytometric analysis of FAIK3-5 cells 24h after treatment with the compound and solvent controls. To set the threshold for dead cells' fluorescence intensities a living-dead control comprising a population of heat-killed FAIK3-5 cells was utilized and all samples were visualized in relation to the control (red). (C) Graphical overview of the data distribution of the proportion of dead cells in different experimental replicates (N=3) for each condition and the untreated control show model based means (black dots) and their 95% confidence intervals. (D) Multiple comparison analysis were conducted based on odds-ratios of treatment means (black dots) that indicate the average chance to obtain dead cells in treatment conditions and the untreated control. Blue bars indicate simultaneous 95% confidence intervals of calculated ratios and p-values for each analysis are displayed on the ride side (see Supporting Information S 13).

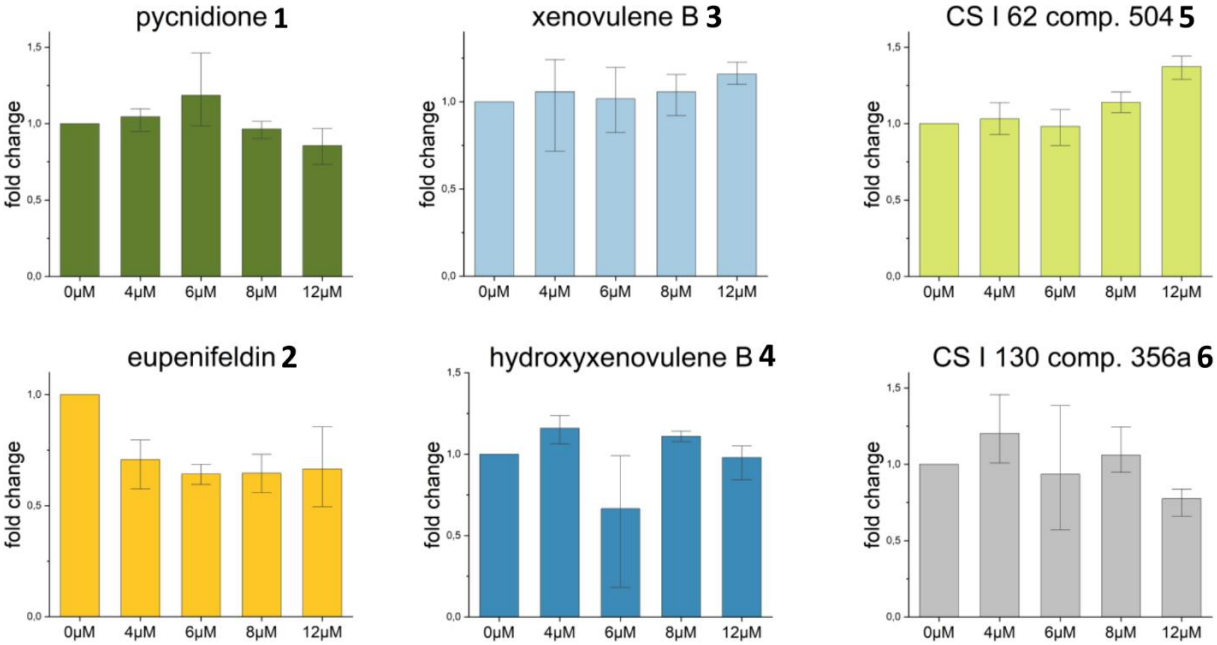

Fig. S8. Assessment of basic erythropoietin concentrations after administration of 4 µM, 6 µM, 8 µM and 12 µM of the tropolone sesquiterpenoids (TS) pycnidione **1**, eupenifeldin **2**, xenovulene B **3**, 4-hydroxyxenovulene B **4** and 4-dehydroxy norpycnidione **5** and the tropolone-moiety lacking compound 4-hydroxy norxenovulene B **6** for 24h (N=1). Initial tests on EPO concentrations were conducted to assess optimal compound concentration und putative concentration dependencies after treatment. Protein concentrations were obtained via ELISA and fold changes compared to the untreated control (0 µM) were calculated. Error bars indicate the standard deviation of the technical replicates (N=3).

2 References

1 Schindelin, J., Arganda-Carreras, I., Frise, E., Kaynig, V., Longair, M., Pietzsch, T., Preibisch, S., Rueden, C., Saalfeld, S., Schmid, B., Tinevez, J.-Y., White, D.J., Hartenstein, V., Eliceiri, K., Tomancak, P., Cardona, A. (2012) Fiji: an open-source platform for biological-image analysis. *Nature methods*, **9** (7), 676–682.

2 Sailem, H.Z., Sero, J.E., Bakal, C. (2015) Visualizing cellular imaging data using PhenoPlot. *Nat Commun*, **6** (1), 5825.

3 Arganda-Carreras, I., Fernández-González, R., Muñoz-Barrutia, A., Ortiz-De-Solorzano, C. (2010) 3D reconstruction of histological sections: Application to mammary gland tissue. *Microscopy research and technique*, **73** (11), 1019–1029.

Supplementary material 9: Cell morphology

Bergmann et al. 2023

Packages used for evaluation

```
library(tidyverse)
library(emmeans)
library(lme4)
library(multcomp)
library(tukeytrend)
library(PerformanceAnalytics)
```

Overview about the data

- Area: Cell area
- Perim.: Perimeter
- AR: Aspect ratio
- Circ.: Circularity
- Solidity: Solidity
- Compound: Treatment of interest
- Plate: Indicator variable for the plates
- Well: Indicator variable for the wells in each plate

```
# First rows of the data set
head(dat)
```

```
##       Area  Perim.    AR Circ. Solidity     Compound Plate           Well
## 1  669.936 177.670 5.926 0.267    0.716 Xenovulene B     1 1:Xenovulene B
## 2 1521.904 257.731 2.988 0.288    0.602 Xenovulene B     1 1:Xenovulene B
## 3  968.534 133.603 1.657 0.682    0.906 Xenovulene B     1 1:Xenovulene B
## 4  537.731 118.493 2.089 0.481    0.768 Xenovulene B     1 1:Xenovulene B
## 5 1103.649 160.116 1.539 0.541    0.817 Xenovulene B     1 1:Xenovulene B
## 6  841.057 125.291 1.084 0.673    0.867 Xenovulene B     1 1:Xenovulene B
```

```r
str(dat)
```

```
## 'data.frame':    300 obs. of  8 variables:
##  $ Area    : num  670 1522 969 538 1104 ...
##  $ Perim.  : num  178 258 134 118 160 ...
##  $ AR      : num  5.93 2.99 1.66 2.09 1.54 ...
##  $ Circ.   : num  0.267 0.288 0.682 0.481 0.541 0.673 0.344 0.313 0.668 0.277 ...
##  $ Solidity: num  0.716 0.602 0.906 0.768 0.817 0.867 0.841 0.665 0.898 0.728 ...
##  $ Compound: Factor w/ 5 levels "Pycnidione","Eupenifeldin",..: 3 3 3 3 3 3 3 3 3 3 ...
##  $ Plate   : Factor w/ 3 levels "1","2","3": 1 1 1 1 1 1 1 1 1 1 ...
##  $ Well    : Factor w/ 15 levels "1:Pycnidione",..: 3 3 3 3 3 3 3 3 3 3 ...
```

Graphical overview about the data set

```r
chart.Correlation(dat[,1:5])
```

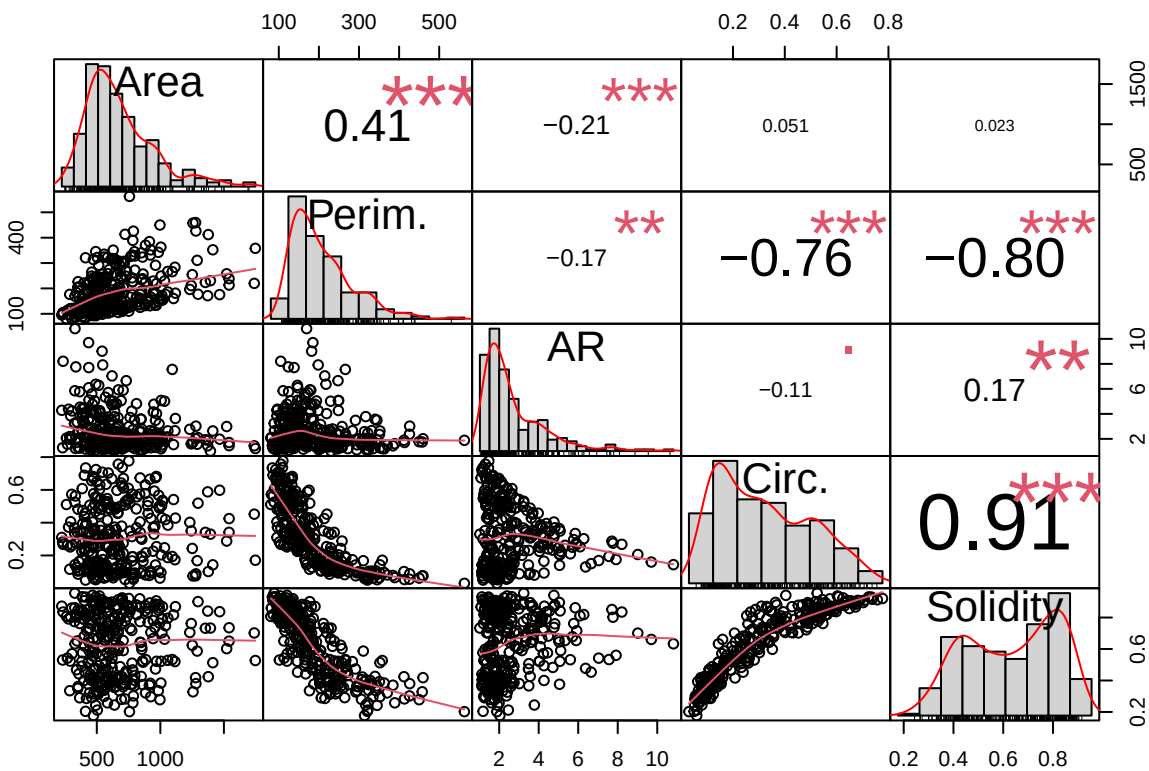

- Area, Perim. and AR are heavily right skewed.
- Modeling will be done on ln-scale for this variables
- The perimeter and the circularity of the cells are highly correlated
- The circularity and the solidity are highly correlated

Modeling

Linear mixed models with compound as fixed and the plates and wells in each plates as random effects.

```
area_fit <- lmer(log(Area) ~ 0 + Compound + (1|Plate) + (1|Well),
                 data=dat)

perim_fit <- lmer(log(Perim.) ~ 0 + Compound + (1|Plate) + (1|Well),
                  data=dat)

AR_fit <- lmer(log(AR) ~ 0 + Compound + (1|Plate) + (1|Well),
               data=dat)

circ_fit <- lmer(Circ. ~ 0 + Compound + (1|Plate) + (1|Well),
                 data=dat)

solidity_fit <- lmer(Solidity ~ 0 + Compound + (1|Plate) + (1|Well),
                     data=dat)
```

Multiple comparisons

Multiple contrast tests are done with respect to the correlations between the dependent variables of the individual models using multiple marginal models.

```
# Contrast matrix
ni <- as.numeric(table(dat$Compound))
cmt <- contrMat(ni, type="Tukey")

# Multiple marginal models
meandiff <- glht(mmm(area_fit=lmer2lm(area_fit),
                     perim_fit=lmer2lm(perim_fit),
                     AR_fit=lmer2lm(AR_fit),
                     circ_fit=lmer2lm(circ_fit),
                     solidity_fit=lmer2lm(solidity_fit)),
                 mlf(cmt))
```

```
fortify(summary(meandiff)) %>%
  mutate(sig=p<0.05) %>%
  dplyr::select(-se, -t)
```

```
##                                     lhs rhs    estimate            p   sig
## area_fit: 2 - 1         area_fit: 2 - 1   0  0.19213995 1.142650e-01 FALSE
## area_fit: 3 - 1         area_fit: 3 - 1   0  0.11959272 8.158089e-01 FALSE
## area_fit: 4 - 1         area_fit: 4 - 1   0  0.27876738 1.060025e-03  TRUE
## area_fit: 5 - 1         area_fit: 5 - 1   0 -0.04066942 9.999970e-01 FALSE
## area_fit: 3 - 2         area_fit: 3 - 2   0 -0.07254723 9.978599e-01 FALSE
## area_fit: 4 - 2         area_fit: 4 - 2   0  0.08662744 9.875405e-01 FALSE
## area_fit: 5 - 2         area_fit: 5 - 2   0 -0.23280937 2.619906e-02  TRUE
## area_fit: 4 - 3         area_fit: 4 - 3   0  0.15917466 4.591904e-01 FALSE
## area_fit: 5 - 3         area_fit: 5 - 3   0 -0.16026214 4.293058e-01 FALSE
## area_fit: 5 - 4         area_fit: 5 - 4   0 -0.31943681 1.521642e-04  TRUE
## perim_fit: 2 - 1       perim_fit: 2 - 1   0  0.21137993 1.635886e-01 FALSE
```

```
## perim_fit: 3 - 1       perim_fit: 3 - 1   0 -0.49524765 8.910007e-10  TRUE
## perim_fit: 4 - 1       perim_fit: 4 - 1   0 -0.47916582 6.004566e-09  TRUE
## perim_fit: 5 - 1       perim_fit: 5 - 1   0 -0.42230986 6.142615e-07  TRUE
## perim_fit: 3 - 2       perim_fit: 3 - 2   0 -0.70662758 0.000000e+00  TRUE
## perim_fit: 4 - 2       perim_fit: 4 - 2   0 -0.69054575 0.000000e+00  TRUE
## perim_fit: 5 - 2       perim_fit: 5 - 2   0 -0.63368979 2.109424e-15  TRUE
## perim_fit: 4 - 3       perim_fit: 4 - 3   0  0.01608183 1.000000e+00 FALSE
## perim_fit: 5 - 3       perim_fit: 5 - 3   0  0.07293779 9.991687e-01 FALSE
## perim_fit: 5 - 4       perim_fit: 5 - 4   0  0.05685595 9.999607e-01 FALSE
## AR_fit: 2 - 1             AR_fit: 2 - 1   0 -0.13656534 9.875647e-01 FALSE
## AR_fit: 3 - 1             AR_fit: 3 - 1   0  0.17582636 8.884248e-01 FALSE
## AR_fit: 4 - 1             AR_fit: 4 - 1   0  0.01227875 1.000000e+00 FALSE
## AR_fit: 5 - 1             AR_fit: 5 - 1   0  0.72034582 2.661694e-10  TRUE
## AR_fit: 3 - 2             AR_fit: 3 - 2   0  0.31239169 8.326036e-02 FALSE
## AR_fit: 4 - 2             AR_fit: 4 - 2   0  0.14884409 9.749516e-01 FALSE
## AR_fit: 5 - 2             AR_fit: 5 - 2   0  0.85691116 7.327472e-14  TRUE
## AR_fit: 4 - 3             AR_fit: 4 - 3   0 -0.16354760 9.376658e-01 FALSE
## AR_fit: 5 - 3             AR_fit: 5 - 3   0  0.54451947 1.054182e-05  TRUE
## AR_fit: 5 - 4             AR_fit: 5 - 4   0  0.70806707 1.138674e-09  TRUE
## circ_fit: 2 - 1         circ_fit: 2 - 1   0 -0.03926667 9.999172e-01 FALSE
## circ_fit: 3 - 1         circ_fit: 3 - 1   0  0.28810000 1.299855e-08  TRUE
## circ_fit: 4 - 1         circ_fit: 4 - 1   0  0.34545000 4.785972e-11  TRUE
## circ_fit: 5 - 1         circ_fit: 5 - 1   0  0.17508333 1.325006e-02  TRUE
## circ_fit: 3 - 2         circ_fit: 3 - 2   0  0.32736667 1.876521e-11  TRUE
## circ_fit: 4 - 2         circ_fit: 4 - 2   0  0.38471667 3.930190e-13  TRUE
## circ_fit: 5 - 2         circ_fit: 5 - 2   0  0.21435000 9.304627e-04  TRUE
## circ_fit: 4 - 3         circ_fit: 4 - 3   0  0.05735000 9.941451e-01 FALSE
## circ_fit: 5 - 3         circ_fit: 5 - 3   0 -0.11301667 4.352890e-01 FALSE
## circ_fit: 5 - 4         circ_fit: 5 - 4   0 -0.17036667 2.845057e-02  TRUE
## solidity_fit: 2 - 1 solidity_fit: 2 - 1   0 -0.04516667 9.966646e-01 FALSE
## solidity_fit: 3 - 1 solidity_fit: 3 - 1   0  0.34365000 3.108624e-15  TRUE
## solidity_fit: 4 - 1 solidity_fit: 4 - 1   0  0.35520000 2.220446e-16  TRUE
## solidity_fit: 5 - 1 solidity_fit: 5 - 1   0  0.27705000 3.567954e-10  TRUE
## solidity_fit: 3 - 2 solidity_fit: 3 - 2   0  0.38881667 0.000000e+00  TRUE
## solidity_fit: 4 - 2 solidity_fit: 4 - 2   0  0.40036667 0.000000e+00  TRUE
## solidity_fit: 5 - 2 solidity_fit: 5 - 2   0  0.32221667 6.716849e-14  TRUE
## solidity_fit: 4 - 3 solidity_fit: 4 - 3   0  0.01155000 1.000000e+00 FALSE
## solidity_fit: 5 - 3 solidity_fit: 5 - 3   0 -0.06660000 9.051454e-01 FALSE
## solidity_fit: 5 - 4 solidity_fit: 5 - 4   0 -0.07815000 7.505367e-01 FALSE
```

Graphical overview about the multiple comparisons

The graphic displays the multiple comparisons on response scale. For the models that run on ln-transformed variables the contrasts and their simultanious 95% confidence intervals are already back transformed to the response scale.
The black horizontal lines indicate the $H_0 : \mu_i - \mu_{i'} = 0$ (for models that were run on response scale) or $H_0 : exp(ln(\mu_i) - ln(\mu_{i'})) = \mu_i/\mu_{i'} = 1$ (for models that were run on ln scale). The contrasts are treated as significantly different from 0 or 1, respectively, if the confidence intervals do not cover the horizontal lines.

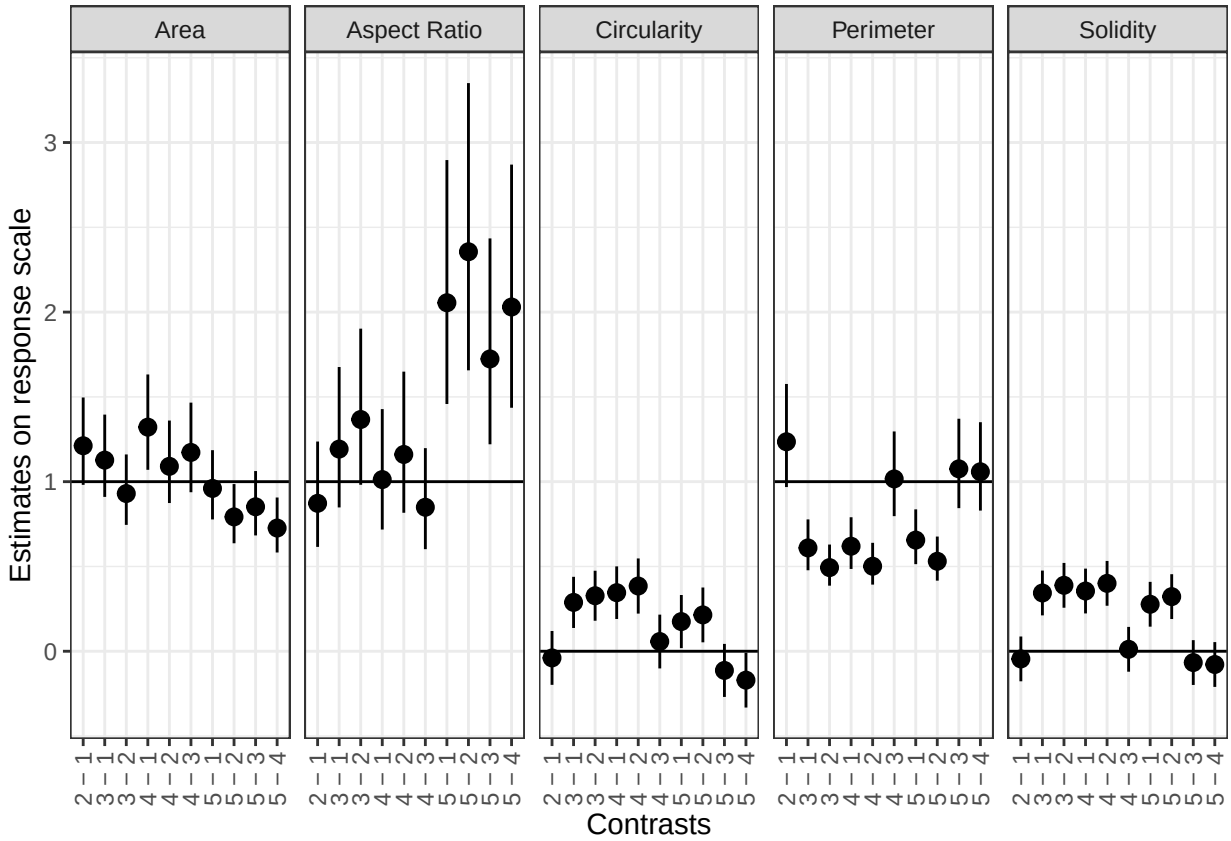

Number code for contrast tests

- 1: Pycnidione
- 2: Eupenifeldin
- 3: Xenovulene B
- 4: 4-hydroxyxenovulene B
- 5: 4-dehydroxy norpycnidione

Supplementary material 10: Branches

Bergmann et al. 2023

Packages used for evaluation

```
library(tidyverse)
library(emmeans)
library(lme4)
library(multcomp)
library(tukeytrend)
library(PerformanceAnalytics)
```

Overview about the data

- Compound: Treatment variable
- Branches: Number of branches
- Junctions: Number of junctions
- Plate: Indicator variable for the plates
- Well: Indicates each well in each plate

```
# First rows of the data set
head(dat)
```

```
##       Compound Branches Junctions Plate           Well
## 1 Xenovulene B        1         0     1 1:Xenovulene B
## 2 Xenovulene B        1         0     1 1:Xenovulene B
## 3 Xenovulene B        5         2     1 1:Xenovulene B
## 4 Xenovulene B        1         0     1 1:Xenovulene B
## 5 Xenovulene B        5         2     1 1:Xenovulene B
## 6 Xenovulene B        1         0     1 1:Xenovulene B
```

```
# Overview about the structure of the data set
str(dat)
```

```
## 'data.frame':    300 obs. of  5 variables:
##  $ Compound : Factor w/ 5 levels "Pycnidione","Eupenifeldin",..: 3 3 3 3 3 3 3 3 3 3 ...
##  $ Branches : int  1 1 5 1 5 1 1 1 8 3 ...
##  $ Junctions: int  0 0 2 0 2 0 0 0 3 1 ...
##  $ Plate    : Factor w/ 3 levels "1","2","3": 1 1 1 1 1 1 1 1 1 1 ...
##  $ Well     : Factor w/ 15 levels "1:Pycnidione",..: 3 3 3 3 3 3 3 3 3 3 ...
```

```r
chart.Correlation(dat[,2:3], method="spearman")
```

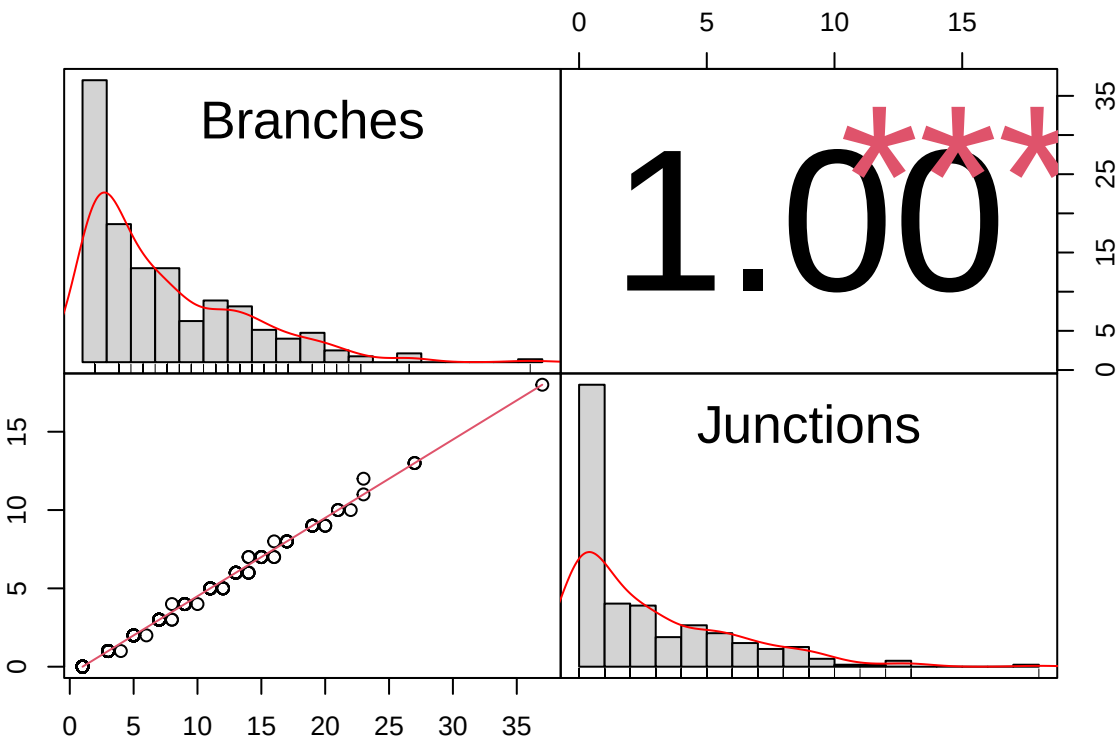

- Both variables are heavily right skewed: Modeling will be done on ln-scale
- Both variables are heavily correlated: Spearman correlation of 0.9988314 (rounded to one in the graphic above)

Modeling

Linear mixed models with compound as fixed and the plates and wells in each plates as random effects. Both dependent variables were ln-transformed. Due to zeros in the variable `Junctions`, a one was added to all observations resulting in a transformed variable $ln(y_i + 1)$.

```r
branch_fit <- lmer(log(Branches) ~ 0 + Compound + (1|Plate) + (1|Well),
            data=dat)

junction_fit <- lmer(log1p(Junctions) ~ 0 + Compound + (1|Plate) + (1|Well),
            data=dat)
```

Multiple comparisons

Multiple contrast tests are done with respect to the correlations between the models using multiple marginal models, since all fife models depend on variables that were measured on the same cells.

```
# Contrast matrix
ni <- as.numeric(table(dat$Compound))
cmt <- contrMat(ni, type="Tukey")

# Multiple marginal models
meandiff <- glht(mmm(branch_fit=lmer2lm(branch_fit),
                     junction_fit=lmer2lm(junction_fit)),
                 mlf(cmt))
```

```
fortify(summary(meandiff)) %>%
        mutate(sig=p<0.05)
```

```
##                                     lhs rhs   estimate        se            t
## branch_fit: 2 - 1     branch_fit: 2 - 1   0  0.3455479 0.1804186   1.91525611
## branch_fit: 3 - 1     branch_fit: 3 - 1   0 -1.4140207 0.1719511  -8.22339004
## branch_fit: 4 - 1     branch_fit: 4 - 1   0 -1.4282047 0.1774193  -8.04988255
## branch_fit: 5 - 1     branch_fit: 5 - 1   0 -1.8374201 0.1790962 -10.25940051
## branch_fit: 3 - 2     branch_fit: 3 - 2   0 -1.7595687 0.1623178 -10.84026818
## branch_fit: 4 - 2     branch_fit: 4 - 2   0 -1.7737527 0.1856251  -9.55556499
## branch_fit: 5 - 2     branch_fit: 5 - 2   0 -2.1829680 0.1815261 -12.02563948
## branch_fit: 4 - 3     branch_fit: 4 - 3   0 -0.0141840 0.1795405  -0.07900169
## branch_fit: 5 - 3     branch_fit: 5 - 3   0 -0.4233993 0.1735750  -2.43928806
## branch_fit: 5 - 4     branch_fit: 5 - 4   0 -0.4092153 0.1846690  -2.21593936
## junction_fit: 2 - 1 junction_fit: 2 - 1   0  0.3099408 0.1305533   2.37405466
## junction_fit: 3 - 1 junction_fit: 3 - 1   0 -1.0883100 0.1269453  -8.57305951
## junction_fit: 4 - 1 junction_fit: 4 - 1   0 -1.1057328 0.1295729  -8.53367121
## junction_fit: 5 - 1 junction_fit: 5 - 1   0 -1.3934873 0.1305520 -10.67381151
## junction_fit: 3 - 2 junction_fit: 3 - 2   0 -1.3982507 0.1229900 -11.36881533
## junction_fit: 4 - 2 junction_fit: 4 - 2   0 -1.4156735 0.1313440 -10.77836099
## junction_fit: 5 - 2 junction_fit: 5 - 2   0 -1.7034280 0.1276343 -13.34616685
## junction_fit: 4 - 3 junction_fit: 4 - 3   0 -0.0174228 0.1280084  -0.13610661
## junction_fit: 5 - 3 junction_fit: 5 - 3   0 -0.3051773 0.1229987  -2.48114292
## junction_fit: 5 - 4 junction_fit: 5 - 4   0 -0.2877545 0.1313428  -2.19086628
##                                p   sig
## branch_fit: 2 - 1   3.284189e-01 FALSE
## branch_fit: 3 - 1   6.661338e-16  TRUE
## branch_fit: 4 - 1   3.774758e-15  TRUE
## branch_fit: 5 - 1   0.000000e+00  TRUE
## branch_fit: 3 - 2   0.000000e+00  TRUE
## branch_fit: 4 - 2   0.000000e+00  TRUE
## branch_fit: 5 - 2   0.000000e+00  TRUE
## branch_fit: 4 - 3   9.999994e-01 FALSE
## branch_fit: 5 - 3   1.136312e-01 FALSE
## branch_fit: 5 - 4   1.870589e-01 FALSE
## junction_fit: 2 - 1 1.334353e-01 FALSE
## junction_fit: 3 - 1 0.000000e+00  TRUE
## junction_fit: 4 - 1 0.000000e+00  TRUE
## junction_fit: 5 - 1 0.000000e+00  TRUE
```

```
## junction_fit: 3 - 2 0.000000e+00  TRUE
## junction_fit: 4 - 2 0.000000e+00  TRUE
## junction_fit: 5 - 2 0.000000e+00  TRUE
## junction_fit: 4 - 3 9.999818e-01 FALSE
## junction_fit: 5 - 3 1.036630e-01 FALSE
## junction_fit: 5 - 4 1.991656e-01 FALSE
```

Graphical overview about the multiple comparisons

The graphic displays the multiple comparisons on response scale. Both models run on ln-transformed variables, but the contrasts and their simultanious 95% confidence intervals are already back transformed to the response scale.
Hence, the black horizontal lines indicate the $H_0 : exp(ln(\mu_i) - ln(\mu_{i'})) = \mu_i/\mu_{i'} = 1$ or $H_0 : exp(ln(\mu_i + 1) - ln(\mu_{i'} + 1)) = /\mu_i + 1)/(\mu_{i'} + 1) = 1$, respectively. The contrasts are treated as significantly different from 1, if the confidence intervals do not cover the horizontal lines.

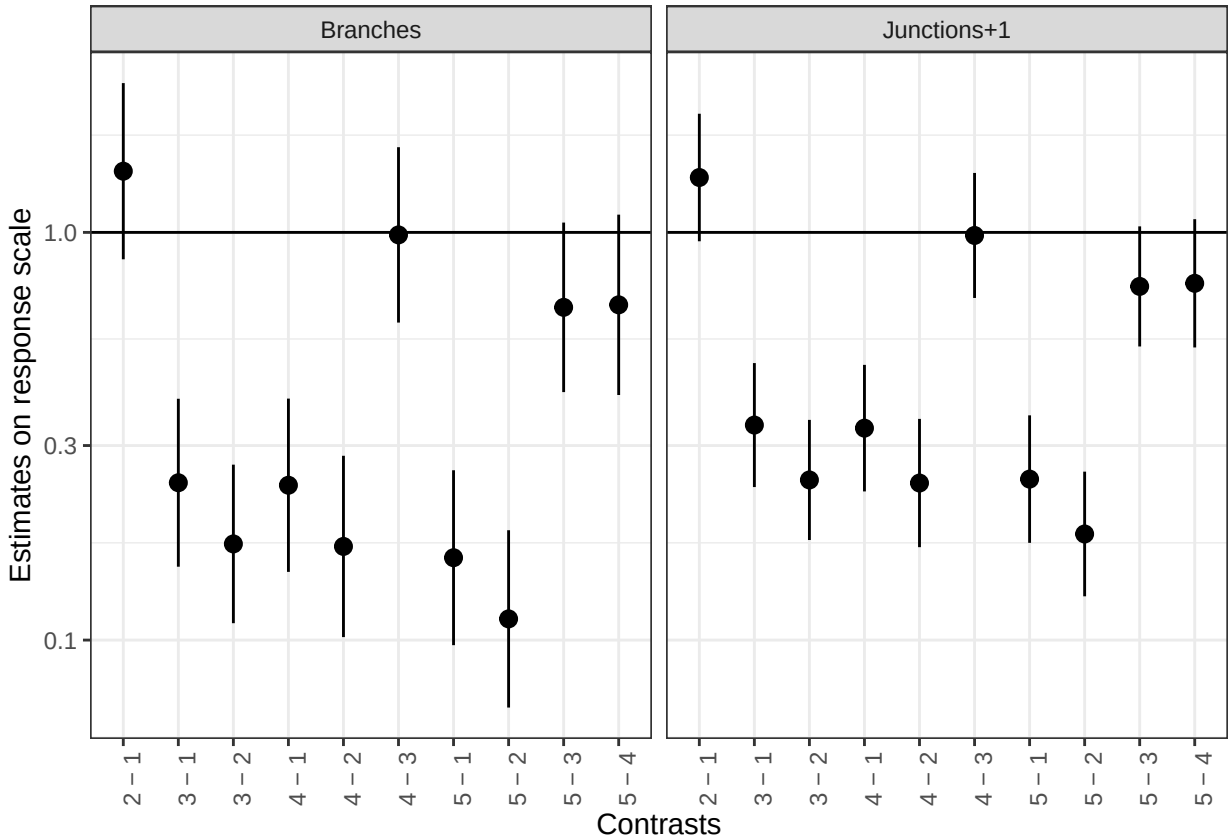

Number code for contrast tests

- 1: Pycnidione
- 2: Eupenifeldin
- 3: Xenovulene B
- 4: 4-hydroxyxenovulene B
- 5: 4-dehydroxy norpycnidione

Supplementary material 11: Proliferation for 4-hydroxy norxenovulene B 6 and DMSO

Bergmann et al. 2023

```
# Load the packages used for evaluation
library(lme4)
library(lmerTest)
library(tidyverse)
library(emmeans)
library(multcomp)
```

Data set

- Treatment: Name of the treatments (combination of compound and dose)
- Rep: Repetition (timepoint)
- Plate: Plate per timepoint
- Prop: Proportion of the fluorescence signals at the start of the experiment and its end
- Fluo1: Fluorescence signals at the start of the experiments (day one)
- Fluo3: Fluorescence signals at the end of the experiments (day three)

```
proli7
```

```
##                        Treatment Rep Plate      Prop Fluo1 Fluo3
## 1                      untreated   1     1 12.220345 33276  2723
## 2   4-hydroxy norxenovulene B 6:4   1     1 12.148959 33276  2739
## 3   4-hydroxy norxenovulene B 6:6   1     1 11.867332 33276  2804
## 4   4-hydroxy norxenovulene B 6:8   1     1 12.052155 33276  2761
## 5  4-hydroxy norxenovulene B 6:12   1     1 11.679888 33276  2849
## 6                      untreated   1     2 12.338154 33276  2697
## 7                       DMSO:0.4   1     2 12.338154 33276  2697
## 8                       DMSO:0.6   1     2 12.078403 33276  2755
## 9                       DMSO:0.8   1     2 12.434978 33276  2676
## 10                      DMSO:1.2   1     2 11.522161 33276  2888
## 11                     untreated   2     3  9.097393 36990  4066
## 12  4-hydroxy norxenovulene B 6:4   2     3  9.153675 36990  4041
## 13  4-hydroxy norxenovulene B 6:6   2     3  8.838710 36990  4185
## 14  4-hydroxy norxenovulene B 6:8   2     3  8.784137 36990  4211
## 15 4-hydroxy norxenovulene B 6:12   2     3  8.534841 36990  4334
## 16                     untreated   2     4  9.097393 36990  4066
## 17                      DMSO:0.4   2     4  9.286970 36990  3983
## 18                      DMSO:0.6   2     4  9.249812 36990  3999
## 19                      DMSO:0.8   2     4  9.097393 36990  4066
## 20                      DMSO:1.2   2     4  8.586351 36990  4308
## 21                     untreated   3     5 11.146008 42444  3808
## 22  4-hydroxy norxenovulene B 6:4   3     5 11.102276 42444  3823
```

```
## 23  4-hydroxy norxenovulene B 6:6   3     5 10.967442 42444  3870
## 24  4-hydroxy norxenovulene B 6:8   3     5 10.154067 42444  4180
## 25 4-hydroxy norxenovulene B 6:12   3     5  9.977433 42444  4254
## 26                      untreated   3     6 11.146008 42444  3808
## 27                       DMSO:0.4   3     6 10.699269 42444  3967
## 28                       DMSO:0.6   3     6 10.767123 42444  3942
## 29                       DMSO:0.8   3     6 10.354721 42444  4099
## 30                       DMSO:1.2   3     6  9.872994 42444  4299
```

Statistical model

- Linear mixed effects model
- Fluorescence proportion as response variable (ln-transformed)
- Repetition and Treatment as fixed effects
- Plates nested in Repetition as normal distributed random effects

```
fit_p7 <- lmer(log(Prop) ~ Rep + Treatment  + (1|Rep:Plate), data=proli7)
```

Model based means and their pointwise 95% confidence intervals

- All mean comparisons were performed on the ln-scale
- The means and their CI are back transformed from the ln-scale to the response scale

```
means <- emmeans(fit_p7,
                 specs="Treatment",
                 type="response")

means
```

```
##                        Treatment  response         SE  lower.CL upper.CL
## 1                      untreated 10.758070 0.09157412 10.566103 10.95353
## 2  4-hydroxy norxenovulene B 6:4 10.728754 0.13274648 10.452111 11.01272
## 3  4-hydroxy norxenovulene B 6:6 10.478912 0.12965520 10.208712 10.75626
## 4  4-hydroxy norxenovulene B 6:8 10.244758 0.12675801  9.980595 10.51591
## 5 4-hydroxy norxenovulene B 6:12  9.982778 0.12351654  9.725370 10.24700
## 6                       DMSO:0.4 10.701854 0.13241364 10.425904 10.98511
## 7                       DMSO:0.6 10.634415 0.13157923 10.360205 10.91588
## 8                       DMSO:0.8 10.540625 0.13041876 10.268833 10.81961
## 9                       DMSO:1.2  9.921181 0.12275441  9.665362 10.18377
```

A graphical overview about this table is given in the Fig. S6 C.

Mean comparisons (contrast tests)

Pairwise mean comparisons, that are defined below by `cont_list`, were run based on mean differences $ln(\hat{\mu}_j) - ln(\hat{\mu}_{j'})$. The tested null-hypothesis for each comparison was $H_0 : ln(\mu_j) - ln(\mu_{j'}) = 0$. The table below shows results from the tests that are already back transformed to the response scale. Hence the back transformed contrasts become proportions on the response scale $exp(ln(\hat{\mu}_j) - ln(\hat{\mu}_{j'})) = \hat{\mu}_j/\hat{\mu}_{j'}$. Similarly, the H_0 for the back transformed contrasts changes to $H_0 : \mu_j/\mu_{j'} = 1$

```r
# List of contrast coefficients
cont_list
```

```
## $`4-hydroxy norxenovulene B 6:4 - untreated`
## [1] -1  1  0  0  0  0  0  0  0
##
## $`4-hydroxy norxenovulene B 6:6 - untreated`
## [1] -1  0  1  0  0  0  0  0  0
##
## $`4-hydroxy norxenovulene B 6:8 - untreated`
## [1] -1  0  0  1  0  0  0  0  0
##
## $`4-hydroxy norxenovulene B 6:12 - untreated`
## [1] -1  0  0  0  1  0  0  0  0
##
## $`DMSO:0.4 - untreated`
## [1] -1  0  0  0  0  1  0  0  0
##
## $`DMSO:0.6 - untreated`
## [1] -1  0  0  0  0  0  1  0  0
##
## $`DMSO:0.8 - untreated`
## [1] -1  0  0  0  0  0  0  1  0
##
## $`DMSO:1.2 - untreated`
## [1] -1  0  0  0  0  0  0  0  1
##
## $`DMSO:0.4 - 4-hydroxy norxenovulene B 6:4`
## [1]  0 -1  0  0  0  1  0  0  0
##
## $`DMSO:0.6 - 4-hydroxy norxenovulene B 6:6`
## [1]  0  0 -1  0  0  0  1  0  0
##
## $`DMSO:0.8 - 4-hydroxy norxenovulene B 6:8`
## [1]  0  0  0 -1  0  0  0  1  0
##
## $`DMSO:1.2 - 4-hydroxy norxenovulene B 6:12`
## [1]  0  0  0  0 -1  0  0  0  1
```

```r
# Multiple contrast tests
comp <- contrast(means,
                 method=cont_list,
                 adjust="mvt")
```

```
##                                     contrast     ratio p.value   sig
## 1  4-hydroxy norxenovulene B 6:12 / untreated 0.9279339   0.001  TRUE
## 2   4-hydroxy norxenovulene B 6:4 / untreated 0.9972749  >0.999 FALSE
## 3   4-hydroxy norxenovulene B 6:6 / untreated 0.9740513   0.522 FALSE
## 4   4-hydroxy norxenovulene B 6:8 / untreated 0.9522858   0.036  TRUE
## 5    DMSO:0.4 / 4-hydroxy norxenovulene B 6:4 0.9974927  >0.999 FALSE
## 6                        DMSO:0.4 / untreated 0.9947745  >0.999 FALSE
## 7    DMSO:0.6 / 4-hydroxy norxenovulene B 6:6 1.0148396   0.981 FALSE
## 8                        DMSO:0.6 / untreated 0.9885058   0.986 FALSE
## 9    DMSO:0.8 / 4-hydroxy norxenovulene B 6:8 1.0288798   0.648 FALSE
## 10                       DMSO:0.8 / untreated 0.9797877   0.775 FALSE
## 11  DMSO:1.2 / 4-hydroxy norxenovulene B 6:12 0.9938297  >0.999 FALSE
## 12                       DMSO:1.2 / untreated 0.9222082  <0.001  TRUE
```

The contrast ratios, their corresponding p-values and their confidence intervals (table below) are shown in Fig. S6 D.

```r
confint(comp)
```

```
##  contrast                                    ratio     SE   df lower.CL upper.CL
##  4-hydroxy norxenovulene B 6:4 / untreated  0.997 0.0147 18.6    0.952    1.045
##  4-hydroxy norxenovulene B 6:6 / untreated  0.974 0.0144 18.6    0.930    1.020
##  4-hydroxy norxenovulene B 6:8 / untreated  0.952 0.0141 18.6    0.909    0.998
##  4-hydroxy norxenovulene B 6:12 / untreated 0.928 0.0137 18.6    0.886    0.972
##  DMSO:0.4 / untreated                       0.995 0.0147 18.6    0.950    1.042
##  DMSO:0.6 / untreated                       0.989 0.0146 18.6    0.944    1.036
##  DMSO:0.8 / untreated                       0.980 0.0145 18.6    0.935    1.027
##  DMSO:1.2 / untreated                       0.922 0.0136 18.6    0.880    0.966
##  DMSO:0.4 / 4-hydroxy norxenovulene B 6:4   0.997 0.0179 17.2    0.942    1.056
##  DMSO:0.6 / 4-hydroxy norxenovulene B 6:6   1.015 0.0182 17.2    0.959    1.074
##  DMSO:0.8 / 4-hydroxy norxenovulene B 6:8   1.029 0.0185 17.2    0.972    1.089
##  DMSO:1.2 / 4-hydroxy norxenovulene B 6:12  0.994 0.0178 17.2    0.939    1.052
##
## Results are averaged over the levels of: Rep
## Degrees-of-freedom method: kenward-roger
## Confidence level used: 0.95
## Conf-level adjustment: mvt method for 12 estimates
## Intervals are back-transformed from the log scale
```

Supplementary material 12: Proliferation

Bergmann et al. 2023

```
# Load the packages used for evaluation
library(tidyverse)
library(emmeans)
library(multcomp)
```

Data set

- Compound: Name of the treatments
- Rep: Repetition (timepoint)
- Prop: Proportions of the fluorescence signals at the start of the experiment and its end
- Fluo1: Fluorescence signals at the start of the experiments (day one)
- Fluo3: Fluorescence signals at the end of the experiments (day three)

```
proli
```

```
##                        Compound Rep      Prop Fluo1 Fluo3
## 1                xenovulene B 3   1  5.611080 59758 10650
## 2                eupenifeldin 2   1  5.509681 59758 10846
## 3  4-dehydroxy norpycnidione 5   1  5.765920 59758 10364
## 4      4-hydroxyxenovulene B 4   1  5.857479 59758 10202
## 5                  pycnidione 1   1  5.870714 59758 10179
## 6  4-hydroxy norxenovulene B 6   1 12.898338 59758  4633
## 7                     untreated   1 14.221323 59758  4202
## 8                xenovulene B 3   2  6.730180 64603  9599
## 9                eupenifeldin 2   2  6.730180 64603  9599
## 10 4-dehydroxy norpycnidione 5   2  6.346694 64603 10179
## 11     4-hydroxyxenovulene B 4   2  7.140820 64603  9047
## 12                 pycnidione 1   2  6.899082 64603  9364
## 13 4-hydroxy norxenovulene B 6   2 14.968258 64603  4316
## 14                    untreated   2 15.888588 64603  4066
## 15               xenovulene B 3   3  6.417296 50164  7817
## 16               eupenifeldin 2   3  9.086035 50164  5521
## 17 4-dehydroxy norpycnidione 5   3  6.590121 50164  7612
## 18     4-hydroxyxenovulene B 4   3  6.796369 50164  7381
## 19                 pycnidione 1   3  7.598304 50164  6602
## 20 4-hydroxy norxenovulene B 6   3 15.178215 50164  3305
## 21                    untreated   3 15.607965 50164  3214
```

Linear model

The data can be treated as a block-design with replicates as blocks and compund as variable of interest.

- Rep as blocks
- Compund as treatments
- Prop (ln-transformed proportions) as dependent variable

```
fit <- lm(log(Prop) ~ Rep + Compound, data=proli)
```

The fitted model is $ln(y_{ij}) = \hat{\mu} + \hat{r}_i + \hat{c}_j + \hat{e}_{ij}$ with:

- $ln(y_{ij})$: Ln-transformed proportions (signal on day 1 / signal on day 3)
- $\hat{\mu}$: Fitted overall mean proportion
- $\hat{r}_i$: Observed effects due to the replication, with $i = 1, 2$
- $\hat{c}_j$: Observed effects of the compounds, with $j = 1, \ldots, 7$
- $\hat{e}_{ij}$: Observed residuals

Analysis of variance

```
anova(fit)
```

```
## Analysis of Variance Table
##
## Response: log(Prop)
##           Df  Sum Sq Mean Sq F value    Pr(>F)
## Rep        2 0.16006 0.08003  13.226 0.0009237 ***
## Compound   6 2.87086 0.47848  79.078 6.044e-09 ***
## Residuals 12 0.07261 0.00605
## ---
## Signif. codes:  0 '***' 0.001 '**' 0.01 '*' 0.05 '.' 0.1 ' ' 1
```

- The compound is significant ($\alpha = 0.05 > p = 6.044e - 09$)

Model based least square means and their pointwise 95% confidence intervals

- All mean comparisons were performed on the ln-scale
- The means and their CI are back transformed from the ln-scale to the response scale

```
means <- emmeans(fit,
                 specs="Compound",
                 type="response")
```

```
##                       Compound  response        SE df  lower.CL  upper.CL
## 1                    untreated 15.221491 0.6835946 12 13.802617 16.786222
## 2                 pycnidione 1  6.751490 0.3032083 12  6.122148  7.445526
## 3               eupenifeldin 2  6.958397 0.3125004 12  6.309768  7.673702
## 4               xenovulene B 3  6.234597 0.2799947 12  5.653438  6.875498
## 5     4-hydroxyxenovulene B 4  6.575245 0.2952931 12  5.962332  7.251163
## 6 4-dehydroxy norpycnidione 5  6.224482 0.2795404 12  5.644266  6.864343
## 7 4-hydroxy norxenovulene B 6 14.310075 0.6426630 12 12.976158 15.781114
```

A graphical overview about this table is given in the manuscript in Fig. 3 A.

Mean comparisons (contrast tests)

Pairwise mean comparisons were run based on mean differences $ln(\hat{\mu}_j) - ln(\hat{\mu}_{j'})$. The tested null-hypothesis for each comparison was $H_0 : ln(\mu_j) - ln(\mu_{j'}) = 0$. The table below shows results from the tests that are already back transformed to the response scale. Hence, the back transformed contrasts become proportions on the response scale $exp(ln(\hat{\mu}_j) - ln(\hat{\mu}_{j'})) = \hat{\mu}_j/\hat{\mu}_{j'}$. Similarly, the H_0 for the back transformed contrasts changes to $H_0 : \mu_j/\mu_{j'} = 1$

```
# Contrasts are given on the response scale
comp <- contrast(means,
                 method="pairwise",
                 adjust="mvt")
```

```
##                                                    contrast ratio p.value
## 1                                    untreated / pycnidione 1  2.25  <0.001
## 2                                  untreated / eupenifeldin 2  2.19  <0.001
## 3                                  untreated / xenovulene B 3  2.44  <0.001
## 4                        untreated / (4-hydroxyxenovulene B 4)  2.31  <0.001
## 5                     untreated / (4-dehydroxy norpycnidione 5)  2.45  <0.001
## 6                     untreated / (4-hydroxy norxenovulene B 6)  1.06   0.951
## 7                                pycnidione 1 / eupenifeldin 2  0.97   0.999
## 8                                pycnidione 1 / xenovulene B 3  1.08    0.86
## 9                      pycnidione 1 / (4-hydroxyxenovulene B 4)  1.03   0.999
## 10                  pycnidione 1 / (4-dehydroxy norpycnidione 5)  1.08   0.849
## 11                  pycnidione 1 / (4-hydroxy norxenovulene B 6)  0.47  <0.001
## 12                              eupenifeldin 2 / xenovulene B 3  1.12   0.611
## 13                    eupenifeldin 2 / (4-hydroxyxenovulene B 4)  1.06   0.967
## 14                eupenifeldin 2 / (4-dehydroxy norpycnidione 5)  1.12   0.597
## 15                eupenifeldin 2 / (4-hydroxy norxenovulene B 6)  0.49  <0.001
## 16                    xenovulene B 3 / (4-hydroxyxenovulene B 4)  0.95   0.976
## 17                xenovulene B 3 / (4-dehydroxy norpycnidione 5)  1.00  >0.999
## 18                xenovulene B 3 / (4-hydroxy norxenovulene B 6)  0.44  <0.001
## 19     (4-hydroxyxenovulene B 4) / (4-dehydroxy norpycnidione 5)  1.06   0.972
## 20     (4-hydroxyxenovulene B 4) / (4-hydroxy norxenovulene B 6)  0.46  <0.001
## 21 (4-dehydroxy norpycnidione 5) / (4-hydroxy norxenovulene B 6)  0.43  <0.001
```

Results of the mean comparisons are summarized in the manuscript in Fig 3 A. The contrast ratios, their corresponding p-values and their confidence intervals (table below) are shown in Fig 3 B in the manuscript.

```r
# 95% simultanious confidence intervals for the contrasts on response scale
confint(contrast(means,
                 method="pairwise",
                 adjust="mvt"))
```

```
##                                                        contrast  LCL  UCL
## 1                                     untreated / pycnidione 1 1.80 2.82
## 2                                   untreated / eupenifeldin 2 1.75 2.73
## 3                                   untreated / xenovulene B 3 1.95 3.05
## 4                         untreated / (4-hydroxyxenovulene B 4) 1.85 2.89
## 5                      untreated / (4-dehydroxy norpycnidione 5) 1.96 3.05
## 6                      untreated / (4-hydroxy norxenovulene B 6) 0.85 1.33
## 7                                 pycnidione 1 / eupenifeldin 2 0.78 1.21
## 8                                 pycnidione 1 / xenovulene B 3 0.87 1.35
## 9                       pycnidione 1 / (4-hydroxyxenovulene B 4) 0.82 1.28
## 10                   pycnidione 1 / (4-dehydroxy norpycnidione 5) 0.87 1.35
## 11                   pycnidione 1 / (4-hydroxy norxenovulene B 6) 0.38 0.59
## 12                               eupenifeldin 2 / xenovulene B 3 0.89 1.39
## 13                     eupenifeldin 2 / (4-hydroxyxenovulene B 4) 0.85 1.32
## 14                 eupenifeldin 2 / (4-dehydroxy norpycnidione 5) 0.89 1.40
## 15                 eupenifeldin 2 / (4-hydroxy norxenovulene B 6) 0.39 0.61
## 16                     xenovulene B 3 / (4-hydroxyxenovulene B 4) 0.76 1.18
## 17                 xenovulene B 3 / (4-dehydroxy norpycnidione 5) 0.80 1.25
## 18                 xenovulene B 3 / (4-hydroxy norxenovulene B 6) 0.35 0.54
## 19     (4-hydroxyxenovulene B 4) / (4-dehydroxy norpycnidione 5) 0.85 1.32
## 20     (4-hydroxyxenovulene B 4) / (4-hydroxy norxenovulene B 6) 0.37 0.57
## 21 (4-dehydroxy norpycnidione 5) / (4-hydroxy norxenovulene B 6) 0.35 0.54
```

Supplementary material 13: Toxicity for 4-hydroxy norxenovulene B 6 and DMSO

Bergmann et al 2023

```r
# Load the packages used for evaluation
library(tidyverse)
library(lme4)
library(lmerTest)
library(emmeans)
library(multcomp)
```

Data set

- Treatment: Name of the treatments (combination compound and dose)
- Rep: Repetition (timepoint)
- Plate: Plate per timepoint
- Prop: Proportion of the dead cells
- Dead: Number of dead cells,
- Alive: Number of living cells
- Total: Total number of cells

```
##                          Treatment Rep Plate Alive        Prop Total Dead
## 1                        untreated   1     1  9968 0.001502554  9983   15
## 2   4-hydroxy norxenovulene B 6:4   1     1  9295 0.069662696  9991  696
## 3   4-hydroxy norxenovulene B 6:6   1     1  9840 0.014916408  9989  149
## 4   4-hydroxy norxenovulene B 6:8   1     1  9627 0.036046861  9987  360
## 5  4-hydroxy norxenovulene B 6:12   1     1  9422 0.055627944  9977  555
## 6                        untreated   1     2  9973 0.001801621  9991   18
## 7                         DMSO:0.4   1     2  9760 0.023023023  9990  230
## 8                         DMSO:0.6   1     2  9161 0.082891180  9989  828
## 9                         DMSO:0.8   1     2  9761 0.021649795  9977  216
## 10                        DMSO:1.2   1     2  9739 0.024441551  9983  244
## 11                       untreated   2     3  9558 0.011275473  9667  109
## 12  4-hydroxy norxenovulene B 6:4   2     3  9379 0.012216956  9495  116
## 13  4-hydroxy norxenovulene B 6:6   2     3  9097 0.017920760  9263  166
## 14  4-hydroxy norxenovulene B 6:8   2     3  8968 0.011245865  9070  102
## 15 4-hydroxy norxenovulene B 6:12   2     3  8547 0.017699115  8701  154
## 16                       untreated   2     4  9374 0.001916525  9392   18
## 17                        DMSO:0.4   2     4  9313 0.013766811  9443  130
## 18                        DMSO:0.6   2     4  9153 0.012940796  9273  120
## 19                        DMSO:0.8   2     4  9448 0.010058676  9544   96
## 20                        DMSO:1.2   2     4  9051 0.022147796  9256  205
## 21                       untreated   3     5  9569 0.002709745  9595   26
## 22  4-hydroxy norxenovulene B 6:4   3     5  9107 0.040863612  9495  388
## 23  4-hydroxy norxenovulene B 6:6   3     5  9105 0.025473617  9343  238
```

```
## 24  4-hydroxy norxenovulene B 6:8   3     5  9425 0.002962023  9453   28
## 25 4-hydroxy norxenovulene B 6:12   3     5  8907 0.033318863  9214  307
## 26                      untreated   3     6  9504 0.003460208  9537   33
## 27                       DMSO:0.4   3     6  9327 0.024270321  9559  232
## 28                       DMSO:0.6   3     6  9261 0.033903609  9586  325
## 29                       DMSO:0.8   3     6  9306 0.015446466  9452  146
## 30                       DMSO:1.2   3     6  8899 0.048540575  9353  454
```

Statistical model

- Generalized linear mixed model
- Avereage proportions of dead cells $\hat{\pi}_j$ are modelled
- Binomial assumption (overdispersed binomial is impossible in `glmer()`)
- Modelling of the response variable was done on logit link $ln(\frac{\hat{\pi}_j}{1-\hat{\pi}_j})$
- Repetition and Treatment as fixed effects
- Plates nested in Repetition as random effects

```
fit_t7 <- glmer(cbind(Dead, Alive) ~ Rep + Treatment + (1|Rep:Plate),
                family="binomial",
                data=tox7_num)
```

Model based means and their pointwise 95% confidence intervals

- Average proportions of des cells $\hat{\pi}_j$

```
means <- emmeans(fit_t7,
                 specs="Treatment",
                 type="response")
```

```
##                        Treatment   prob     SE asymp.LCL asymp.UCL
## 1                      untreated 0.0033 0.0005    0.0025    0.0044
## 4  4-hydroxy norxenovulene B 6:8 0.0119 0.0018    0.0088    0.0160
## 3  4-hydroxy norxenovulene B 6:6 0.0134 0.0020    0.0100    0.0180
## 8                       DMSO:0.8 0.0194 0.0029    0.0144    0.0260
## 6                       DMSO:0.4 0.0249 0.0037    0.0186    0.0334
## 5 4-hydroxy norxenovulene B 6:12 0.0252 0.0037    0.0189    0.0336
## 2  4-hydroxy norxenovulene B 6:4 0.0291 0.0042    0.0219    0.0387
## 9                       DMSO:1.2 0.0384 0.0056    0.0289    0.0510
## 7                       DMSO:0.6 0.0536 0.0076    0.0405    0.0706
```

A graphical overview about this table is given in the manuscript in Fig. S7 C.

Multiple comparisons

Pairwise mean comparisons, that are defined below by `cont_list`, were run based on log odds-ratios $ln(\frac{\hat{\pi}_j}{1-\hat{\pi}_j}/\frac{\hat{\pi}_{j'}}{1-\hat{\pi}_{j'}}) = ln(\frac{\hat{\pi}_j}{1-\hat{\pi}_j}) - ln(\frac{\hat{\pi}_{j'}}{1-\hat{\pi}_{j'}})$. The tested null-hypothesis for each comparison was $H_0 : ln(\frac{\pi_j}{1-\pi_j}) - ln(\frac{\pi_{j'}}{1-\pi_{j'}}) = 0$.

```r
# List of contrast coefficients
cont_list
```

```
## $`4-hydroxy norxenovulene B 6:4 - untreated`
## [1] -1  1  0  0  0  0  0  0  0
##
## $`4-hydroxy norxenovulene B 6:6 - untreated`
## [1] -1  0  1  0  0  0  0  0  0
##
## $`4-hydroxy norxenovulene B 6:8 - untreated`
## [1] -1  0  0  1  0  0  0  0  0
##
## $`4-hydroxy norxenovulene B 6:12 - untreated`
## [1] -1  0  0  0  1  0  0  0  0
##
## $`DMSO:0.4 - untreated`
## [1] -1  0  0  0  0  1  0  0  0
##
## $`DMSO:0.6 - untreated`
## [1] -1  0  0  0  0  0  1  0  0
##
## $`DMSO:0.8 - untreated`
## [1] -1  0  0  0  0  0  0  1  0
##
## $`DMSO:1.2 - untreated`
## [1] -1  0  0  0  0  0  0  0  1
##
## $`DMSO:0.4 - 4-hydroxy norxenovulene B 6:4`
## [1]  0 -1  0  0  0  1  0  0  0
##
## $`DMSO:0.6 - 4-hydroxy norxenovulene B 6:6`
## [1]  0  0 -1  0  0  0  1  0  0
##
## $`DMSO:0.8 - 4-hydroxy norxenovulene B 6:8`
## [1]  0  0  0 -1  0  0  0  1  0
##
## $`DMSO:1.2 - 4-hydroxy norxenovulene B 6:12`
## [1]  0  0  0  0 -1  0  0  0  1
```

The table below shows results from the tests that are back transformed to the response scale. Hence the back transformed contrasts become proportions on the response scale $exp[ln(\frac{\hat{\pi}_j}{1-\hat{\pi}_j}) - ln(\frac{\hat{\pi}_{j'}}{1-\hat{\pi}_{j'}})] = \frac{\hat{\pi}_j}{1-\hat{\pi}_j} / \frac{\hat{\pi}_{j'}}{1-\hat{\pi}_{j'}}$. Similarly, the H_0 for the back transformed contrasts changes to $H_0 : \frac{\pi_{j'}}{1-\pi_{j'}} / \frac{\pi_{j'}}{1-\pi_{j'}} = 1$

```r
# Multiple contrast tests
comp <- contrast(means,
                 method=cont_list,
                 adjust="mvt")
```

```
##                                     contrast odds.ratio p.value   sig
## 1  4-hydroxy norxenovulene B 6:12 / untreated  7.7557037  <0.001  TRUE
## 2   4-hydroxy norxenovulene B 6:4 / untreated  8.9839760  <0.001  TRUE
## 3   4-hydroxy norxenovulene B 6:6 / untreated  4.0712481  <0.001  TRUE
## 4   4-hydroxy norxenovulene B 6:8 / untreated  3.6005985  <0.001  TRUE
## 5    DMSO:0.4 / 4-hydroxy norxenovulene B 6:4  0.8528535   0.819 FALSE
## 6                        DMSO:0.4 / untreated  7.6620153  <0.001  TRUE
## 7    DMSO:0.6 / 4-hydroxy norxenovulene B 6:6  4.1679982  <0.001  TRUE
## 8                        DMSO:0.6 / untreated 16.9689545  <0.001  TRUE
## 9    DMSO:0.8 / 4-hydroxy norxenovulene B 6:8  1.6423417   0.031  TRUE
## 10                       DMSO:0.8 / untreated  5.9134131  <0.001  TRUE
## 11  DMSO:1.2 / 4-hydroxy norxenovulene B 6:12  1.5441243    0.06 FALSE
## 12                       DMSO:1.2 / untreated 11.9757703  <0.001  TRUE
```

A graphical overview about this table is given in the manuscript in Fig. S7 D.

Supplementary material 14: Toxicity

Bergmann et al. 2023

```
# Load the packages used for evaluation
library(tidyverse)
library(emmeans)
```

Data set

- Compound: Name of the treatments
- Rep: Repetition (timepoint)
- Total: Total number of cells
- Dead: Number of dead cells
- Prop: Proportion of dead cells (for plotting only)

```
toxy
```

```
##    Rep                     Compound Total Dead Alive        Prop
## 1    1              xenovulene B 3  9520  963  8557 0.101155462
## 2    1              eupenifeldin 2  9358 1431  7927 0.152917290
## 3    1 4-dehydroxy norpycnidione 5  9675  516  9159 0.053333333
## 4    1     4-hydroxyxenovulene B 4  9240 1937  7303 0.209632035
## 5    1                pycnidione 1  9370 1661  7709 0.177267876
## 6    1 4-hydroxy norxenovulene B 6  9611  695  8916 0.072312975
## 7    1                   untreated  9751   51  9700 0.005230233
## 8    2              xenovulene B 3  8951 1000  7951 0.111719361
## 9    2              eupenifeldin 2  9451 1557  7894 0.164744471
## 10   2 4-dehydroxy norpycnidione 5  8932  411  8521 0.046014330
## 11   2     4-hydroxyxenovulene B 4  9261  729  8532 0.078717201
## 12   2                pycnidione 1  9164 1694  7470 0.184853776
## 13   2 4-hydroxy norxenovulene B 6  9354  326  9028 0.034851400
## 14   2                   untreated  9382   33  9349 0.003517374
## 15   3              xenovulene B 3  9585  886  8699 0.092436098
## 16   3              eupenifeldin 2  9767 2313  7454 0.236817856
## 17   3 4-dehydroxy norpycnidione 5  9700  411  9289 0.042371134
## 18   3     4-hydroxyxenovulene B 4  9519  786  8733 0.082571699
## 19   3                pycnidione 1  9342 2442  6900 0.261400128
## 20   3 4-hydroxy norxenovulene B 6  9779  280  9499 0.028632785
## 21   3                   untreated  9772  136  9636 0.013917315
```

Statistical model

- Block design: One observation per compound in each replication
- Generalized linear model
- Binomial proportion for dead cells depend on Rep and Compound
- Logit-Link

```
fit <-  glm(cbind(Dead, Alive) ~ Rep + Compound,
            family=quasibinomial(link="logit"),
            data=toxy)
```

```
summary(fit)$dispersion
```

```
## [1] 129.9988
```

- Huge amound of overdispersion:
- The variance is almost 130 times higher than under simple binomial distribution

Deviance analysis

- Deviance analysis based on F-Test due to quasi-binomial assumption

```
anova(fit,
      test="F")
```

```
## Analysis of Deviance Table
##
## Model: quasibinomial, link: logit
##
## Response: cbind(Dead, Alive)
##
## Terms added sequentially (first to last)
##
##
##          Df Deviance Resid. Df Resid. Dev       F    Pr(>F)
## NULL                        20    13351.9
## Rep       2    178.2        18    13173.7  0.6855    0.5225
## Compound  6  11645.6        12     1528.1 14.9304 6.148e-05 ***
## ---
## Signif. codes:  0 '***' 0.001 '**' 0.01 '*' 0.05 '.' 0.1 ' ' 1
```

- The p-value for the variable compound is far smaller than $\alpha = 0.05$
- At least two compounds differ from each other with regard to their average proportion of dead cells

Estimated average proportions and their comparisons

Pairwise comparisons of average proportions $\hat{\pi}_j$ were run on logit scale. Hence, the tested null-hypothesis for each comparison was $H_0 : ln(\frac{\pi_j}{1-\pi_j}) - ln(\frac{\pi_{j'}}{1-\pi_{j'}}) = 0$. Back transformation to the response scale results in odds ratios $\frac{\hat{\pi}_j}{1-\hat{\pi}_j} / \frac{\hat{\pi}_{j'}}{1-\hat{\pi}_{j'}}$. Hence, back transformation from logit to response scale alters the H_0 such that $H_0 : \frac{\pi_j}{1-\pi_j} / \frac{\pi_{j'}}{1-\pi_{j'}} = 1$.

```
comp <- emmeans(fit,
                specs="Compound",
                contr="pairwise",
                type="response",
                adjust="mvt")
```

Estimated mean proportions of dead cells

```
##                       Compound        prob          SE  df  asymp.LCL  asymp.UCL
## 1                    untreated 0.007550266 0.005782888 Inf 0.00167346 0.03337510
## 2                 pycnidione 1 0.207168230 0.027687215 Inf 0.15809553 0.26664871
## 3               eupenifeldin 2 0.184836578 0.026188748 Inf 0.13888478 0.24172426
## 4               xenovulene B 3 0.100795816 0.020458394 Inf 0.06718123 0.14855122
## 5     4-hydroxyxenovulene B 4 0.122629081 0.022328644 Inf 0.08513631 0.17350178
## 6 4-dehydroxy norpycnidione 5 0.046832482 0.014268929 Inf 0.02558786 0.08419170
## 7 4-hydroxy norxenovulene B 6 0.044942643 0.013896502 Inf 0.02434141 0.08152277
```

A graphical overview about this table is given in the manuscript in Fig. 4 A.

Mean comparisons (contrast tests)

```
##                                                        contrast ratio p.value
## 1                                     untreated / pycnidione 1 0.029  <0.001
## 2                                   untreated / eupenifeldin 2 0.034  <0.001
## 3                                   untreated / xenovulene B 3 0.068   0.012
## 4                         untreated / (4-hydroxyxenovulene B 4) 0.054   0.004
## 5                      untreated / (4-dehydroxy norpycnidione 5) 0.155   0.252
## 6                      untreated / (4-hydroxy norxenovulene B 6) 0.162   0.281
## 7                                 pycnidione 1 / eupenifeldin 2 1.152   0.997
## 8                                 pycnidione 1 / xenovulene B 3 2.331   0.036
## 9                      pycnidione 1 / (4-hydroxyxenovulene B 4) 1.870   0.201
## 10                  pycnidione 1 / (4-dehydroxy norpycnidione 5) 5.318  <0.001
## 11                  pycnidione 1 / (4-hydroxy norxenovulene B 6) 5.553  <0.001
## 12                              eupenifeldin 2 / xenovulene B 3 2.023    0.15
## 13                    eupenifeldin 2 / (4-hydroxyxenovulene B 4) 1.622   0.525
## 14                eupenifeldin 2 / (4-dehydroxy norpycnidione 5) 4.615  <0.001
## 15                eupenifeldin 2 / (4-hydroxy norxenovulene B 6) 4.819  <0.001
## 16                    xenovulene B 3 / (4-hydroxyxenovulene B 4) 0.802    0.99
## 17                xenovulene B 3 / (4-dehydroxy norpycnidione 5) 2.281   0.319
## 18                xenovulene B 3 / (4-hydroxy norxenovulene B 6) 2.382   0.269
## 19     (4-hydroxyxenovulene B 4) / (4-dehydroxy norpycnidione 5) 2.845   0.076
## 20     (4-hydroxyxenovulene B 4) / (4-hydroxy norxenovulene B 6) 2.970    0.06
## 21 (4-dehydroxy norpycnidione 5) / (4-hydroxy norxenovulene B 6) 1.044  >0.999
```

A graphical overview about this table is given in the manuscript in Fig. 4 B.

Supplementary material 15: Proteins

Bergmann et al. 2023

```
# Load the packages used for evaluation
library(tidyverse)
library(lme4)
library(lmerTest)
library(tidyverse)
library(emmeans)
```

Overview about the data

Description of the variables

- Rep: Replication
- Plate: Plate in each replication
- Well: Well in each plate in each replication
- Compund: Chemical compounds (treatment variable)
- Protein: Protein content in pg/ml

```
# First six rows of the data set
head(prote)
```

```
##   Rep Plate Well       Compound  Protein
## 1   1     1    1   pycnidione 1 5.819760
## 2   1     1    1   pycnidione 1 4.158405
## 3   1     1    1   pycnidione 1 4.302978
## 4   1     1    2 xenovulene B 3 7.161895
## 5   1     1    2 xenovulene B 3 6.590697
## 6   1     1    2 xenovulene B 3 7.172868
```

```
# 69 observations at all (rows)
str(prote)
```

```
## 'data.frame':    69 obs. of  5 variables:
##  $ Rep     : Factor w/ 3 levels "1","2","3": 1 1 1 1 1 1 1 1 1 1 ...
##  $ Plate   : Factor w/ 2 levels "1","2": 1 1 1 1 1 1 1 1 1 1 ...
##  $ Well    : Factor w/ 6 levels "1","2","3","4",..: 1 1 1 2 2 2 3 3 3 4 ...
##  $ Compound: Factor w/ 8 levels "DMSO 0.6 % (v/v)",..: 3 3 3 5 5 5 4 4 4 7 ...
##  $ Protein : num  5.82 4.16 4.3 7.16 6.59 ...
```

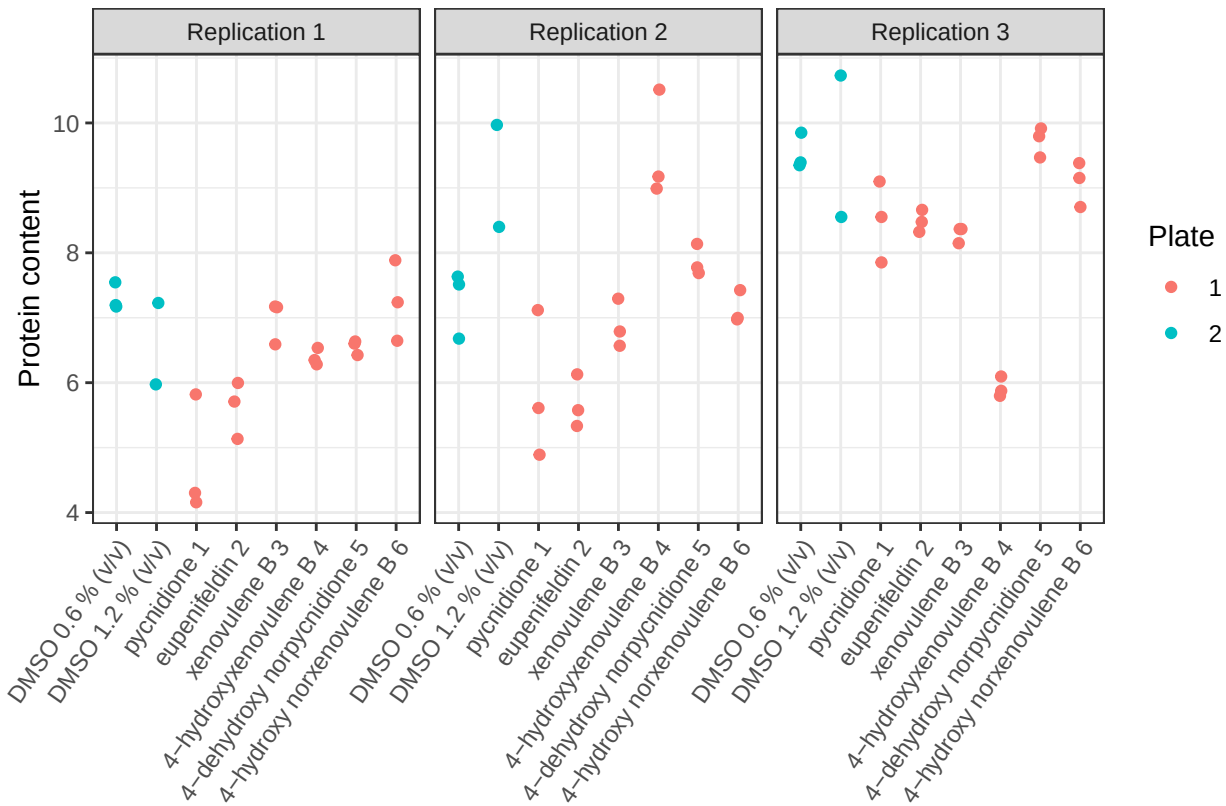

Statistical model

Hierarchical experimental design, since the plates are nested in the replications and the wells are nested in each plate.

- Linear mixed model
- Protein as response variable
- Compounds as fixed effects
- Rep, Plates and Wells as random effects

```
fit <- lmer(Protein ~ Compound + (1|Rep) + (1|Rep:Plate) + (1|Rep:Plate:Well),
            data=prote)
```

Estimated variance components

```
print(VarCorr(fit),comp=c("Variance"),digits=2)
```

```
##  Groups          Name        Variance
##  Rep:Plate:Well  (Intercept) 1.2e+00
##  Rep:Plate       (Intercept) 1.5e-09
##  Rep             (Intercept) 9.7e-01
##  Residual                    4.0e-01
```

- Most of the total variance can be explained by the wells.

- The plates do not explain any variance

```
anova(fit,
      ddf="Kenward-Roger")
```

```
## Type III Analysis of Variance Table with Kenward-Roger's method
##          Sum Sq Mean Sq NumDF  DenDF F value Pr(>F)
## Compound 3.3223 0.47462     7 10.514  1.1038 0.4261
```

- The p-value of 0.4261 is bigger than $\alpha = 0.05$
- No different mean protein contents between the compounds

Supplementary material 16: Proteins after 5-Azacytidine treatment

Bergmann et al. 2023

```r
# Load the packages used for evaluation
library(tidyverse)
library(lme4)
library(lmerTest)
library(tidyverse)
library(emmeans)
library(multcomp)
```

Overview about the data

Description of the variables

- Rep: Replication
- Plate: Plate in each replication
- Well: Well in each plate in each replication
- Compund: Chemical compounds (treatment variable)
- Protein: Protein content in pg/ml

```r
# First six rows of the data set
head(aza)
```

```
##   Rep Plate Well       Compound  Protein
## 1   1     1    1   pycnidione 1 22.10247
## 2   1     1    1   pycnidione 1 19.06987
## 3   1     1    1   pycnidione 1 18.17886
## 4   1     1    2 xenovulene B 3 17.96557
## 5   1     1    2 xenovulene B 3 14.10570
## 6   1     1    2 xenovulene B 3 17.36827
```

```r
# 72 observations at all (rows)
str(aza)
```

```
## 'data.frame':    72 obs. of  5 variables:
##  $ Rep     : Factor w/ 3 levels "1","2","3": 1 1 1 1 1 1 1 1 1 1 ...
##  $ Plate   : Factor w/ 2 levels "1","2": 1 1 1 1 1 1 1 1 1 1 ...
##  $ Well    : Factor w/ 6 levels "1","2","3","4",..: 1 1 1 2 2 2 3 3 3 4 ...
##  $ Compound: Factor w/ 8 levels "DMSO 0.6 % (v/v)",..: 3 3 3 5 5 5 4 4 4 7 ...
##  $ Protein : num  22.1 19.1 18.2 18 14.1 ...
```

Statistical model

Hierarchical experimental design, since the plates are nested in the replications and the wells are nested in each plate.

- Linear mixed model
- Protein as response variable
- Compounds as fixed effects
- Rep, Plates and Wells as random effects

```
fit <- lmer(Protein ~ Compound + (1|Rep) + (1|Rep:Plate) + (1|Rep:Plate:Well),
            data=aza)
```

Estimated variance components

```
print(VarCorr(fit),comp=c("Variance"),digits=2)
```

```
##  Groups         Name        Variance
##  Rep:Plate:Well (Intercept) 0.26
##  Rep:Plate      (Intercept) 0.24
##  Rep            (Intercept) 0.13
##  Residual                   3.96
```

- The residual variance is relatively high, compared to the variance that can be explained due to the experimental design.

```
anova(fit,
      ddf="Kenward-Roger")
```

```
## Type III Analysis of Variance Table with Kenward-Roger's method
##          Sum Sq Mean Sq NumDF  DenDF F value   Pr(>F)
## Compound 160.94  22.991     7 10.845  5.3773 0.007245 **
## ---
## Signif. codes:  0 '***' 0.001 '**' 0.01 '*' 0.05 '.' 0.1 ' ' 1
```

- The p-value of 0.007245 is smaller than $\alpha = 0.05$

Model based least square means and their 95 % confidence intervals

```
means <- emmeans(fit,
                 specs="Compound",
                 adjust="mvt",
                 type="response")
```

```
means
```

```
##  Compound                    emmean    SE   df lower.CL upper.CL
##  DMSO 0.6 % (v/v)              16.9 0.807 14.5     14.4     19.5
##  DMSO 1.2 % (v/v)              18.9 0.807 14.5     16.3     21.4
##  pycnidione 1                  17.8 0.807 14.5     15.3     20.4
##  eupenifeldin 2                13.4 0.807 14.5     10.9     15.9
##  xenovulene B 3                15.1 0.807 14.5     12.5     17.6
##  4-hydroxyxenovulene B 4       14.0 0.807 14.5     11.4     16.5
##  4-dehydroxy norpycnidione 5   15.0 0.807 14.5     12.4     17.5
##  4-hydroxy norxenovulene B 6   15.5 0.807 14.5     13.0     18.1
##
## Degrees-of-freedom method: kenward-roger
## Confidence level used: 0.95
## Conf-level adjustment: mvt method for 8 estimates
```

A graphical overview about this table is given in Fig. 5 C.

Mean comparisons

Only the mean comparisons defined in the list below were tested

```
cont_list
```

```
## $`DMSO 0.6 % (v/v) - pycnidione 1`
## [1]  1  0 -1  0  0  0  0  0
##
## $`DMSO 0.6 % (v/v) - eupenifeldin 2`
## [1]  1  0  0 -1  0  0  0  0
##
## $`DMSO 0.6 % (v/v) - xenovulene B 3`
## [1]  1  0  0  0 -1  0  0  0
##
## $`DMSO 0.6 % (v/v) - 4-hydroxy norxenovulene B 6`
## [1]  1  0  0  0  0  0  0 -1
##
## $`DMSO 1.2 % (v/v) - 4-hydroxyxenovulene B 4`
## [1]  0  1  0  0  0 -1  0  0
##
## $`DMSO 1.2 % (v/v) - 4-dehydroxy norpycnidione 5`
## [1]  0  1  0  0  0  0 -1  0
```

```
comp <- contrast(means,
                 method=cont_list,
                 adjust="mvt")
```

```
comp
```

```
##                                          contrast   estimate p.value   sig
## 1 DMSO 0.6 % (v/v) - 4-hydroxy norxenovulene B 6  1.4027470   0.669 FALSE
## 2              DMSO 0.6 % (v/v) - eupenifeldin 2  3.5509246   0.046  TRUE
## 3                DMSO 0.6 % (v/v) - pycnidione 1 -0.8899113   0.919 FALSE
## 4              DMSO 0.6 % (v/v) - xenovulene B 3  1.8763319   0.418 FALSE
## 5 DMSO 1.2 % (v/v) - 4-dehydroxy norpycnidione 5  3.9179278   0.028  TRUE
## 6     DMSO 1.2 % (v/v) - 4-hydroxyxenovulene B 4  4.9004060   0.008  TRUE
```

A graphical overview about this table is given in Fig. 5 D.